Characterization of Far-Infrared Polar Spectral Signatures for PREFIRE

by

Cassidy Johnson

A thesis submitted in partial fulfillment of

the requirements for the degree of

Master of Science

(Atmospheric Sciences)

at the

UNIVERSITY OF WISCONSIN-MADISON

2023

Abstract

Characterization of Far-Infrared Polar Spectral Signatures for PREFIRE
By Cassidy Johnson

Understanding polar spectral responses in the far-infrared spectrum is crucial to fully characterize Earth's global energy balance. The poles emit more outgoing longwave radiation than they receive through solar radiation and through global transport, however, there is a lack of polar measurements in the far-infrared portion of the longwave spectrum, specifically for wavelengths longer than 15 μm. The Polar Radiant Energy in the Far-Infrared Experiment (PREFIRE) mission will launch two CubeSats in May of 2024 to measure spectrally resolved radiances between 5 and 55 μm, filling this gap in measurements. Using a principal component-based radiative transfer model, the data from PREFIRE is simulated and analyzed on annual and seasonal timescales at three specific locations that have surface observations: Dismal Island (Antarctic coastal), Dome C II (Antarctic inland), and Summit (Greenland inland). Case studies including surface type changes, inversions, and cloud presence are also simulated and analyzed. The results show that the amount of moisture at these locations impacts the expected magnitude of variability across the PREFIRE far-infrared spectrum for annual variability and surface type changes. The spectrum is found to be sensitive to cloud presence, phase, varying effective radii, and optical depths to various magnitudes at each location.

Acknowledgments

Tristan L’Ecuyer: For taking me on as a graduate student on the PREFIRE team, mentoring me, and shaping me to be a better scientist.

Nate Miller: For teaching me how to use the principal component-based radiative transfer model and helping me debug code.

AMRDC: For providing data for this project and giving me an opportunity to do research during my undergraduate career.

The PREFIRE team.

Friends and colleagues in the Department of Atmospheric and Oceanic Sciences.

My supportive parents, brother and sister, friends, and family.

Contents

1 Background

1.1 Polar Climates

Expanding on observations in harsh polar regions is crucial to gain a full picture of Earth's global energy balance. Despite receiving minimal solar energy input due to the steep angle at which the sun illuminates them, these high-latitude areas are a substantial source of Earth's emitted longwave radiation. This longwave emission significantly outweighs the shortwave energy that they receive. Without heat transport from lower latitudes to reestablish equilibrium, polar regions would continuously cool, driven by their emission of more longwave energy than they gain from solar input. According to L'Ecuyer et al. 2015 – a study that reconstructed the global energy budgets based on 21st-century satellite observations – it is estimated that the Arctic emits 2.4 times the energy it receives from the sun and the Antarctic emits 2.8 times the energy received. In the absence of global heat transport, this would cause a net energy deficit exceeding a petawatt in polar regions (L'Ecuyer et al. 2021). It is necessary to characterize the longwave energy balance fully and accurately in polar regions due to their remote and ever-evolving climates.

Anthropogenic climate change can ultimately impact polar regions, which would in turn impact the rest of the globe, causing a warming feedback effect. Temperature increases at lower latitudes caused by anthropogenic warming drive higher temperatures in polar regions within both the atmosphere and oceans. These changes also lead to the consequential thawing of sea ice, snow cover, and retreat of glaciers. Snow cover is especially important to consider when it comes to melting. Normally, the snow present on the Greenland and Antarctic ice sheets is very fine and dry and can reflect up to 85% of shortwave solar energy (Konzelmann & Ohmura 1995). However, when the snow melts, it merges together and becomes wetter which affects its optical longwave

emission properties and will reduce how much sunlight it can reflect and absorb, especially in the far-infrared portion of the spectrum. Larger clumps of wet snow absorb more energy in the longwave infrared portion of the radiation spectrum, and this process can ultimately intensify the melting rate and cause a snow melt-feedback loop (Box et al. 2012; Irannezhad, Ahmadi, & Marttila 2022). Another feedback loop that is cause for concern is the ice-albedo-temperature feedback effect which is caused by melting sea ice.

Throughout the satellite observational record, there have been clear signs of Arctic sea ice decline, especially during summer months, and it is occurring much quicker than models previously predicted (Meier et al. 2014; Parkinson 2019). The loss of approximately 50% of summer ice extent has already had clear effects on the climate: polar amplification occurring due to the ice-albedo-temperature feedback effect, the increase of ocean heat storage which reduces the thickness that new sea ice can achieve, and the decrease in large-scale westerlies in atmospheric circulation (Walsh 2013). While Arctic sea ice decline has been a topic of study for decades, the Antarctic sea ice reduction has only become a topic of discussion in recent years.

Since the beginning of satellite observations in the 1960s, there has been a general increase in Antarctic sea ice extent with record increases from 2012 to 2014 (Eayrs et al. 2019; Parkinson 2019). This abruptly changed from 2014 to 2018 when the Antarctic sea ice extent decreased with decay rates exceeding Arctic sea ice decay rates with record decay through 2018 (Eayrs 2019; Parkinson 2019). This is significant to global energy balance because with less sea ice comes less reflection of solar radiation, and thus more warming of ocean temperatures in the ice-albedo-temperature feedback. On a global scale, the reduction of sea ice in both Antarctica and the Arctic can cause higher occurrences of temperature, precipitation, and extreme weather event anomalies (Walsh 2013).

Understanding the role of emitted radiation in polar regions where sea ice is changing is crucial to gain insight into polar energy balance dynamics, especially in the far-infrared portion of the longwave electromagnetic spectrum.

1.2 The Far-Infrared

Over 99% of global longwave emission occurs between wavelengths of 4 μm and 100 μm. The far-infrared longwave portion of the emission spectrum, defined in this paper as wavelengths longer than 15 μm, accounts for over half of the emitted radiation in polar regions. This definition is consistent with Harries et al. 2008, a study that characterized the importance of far-infrared measurements in relation to Earth's energy balance. The far-infrared spectrum is responsible for a large portion of water vapor, carbon dioxide, and cloud (especially ice) absorption. While there have been many studies and measurements made in the mid-infrared wavelength range (5 to 15 μm) (Ackerman et al. 2019), spectral regions beyond 15 μm have been underexplored. Understanding the cooler, lower-energy far-infrared spectral region is essential for gaining insights into the unique thermal dynamics and climate sensitivity of polar environments.

The study done by Harries et al. 2008 goes on to say that having measurements in the far-infrared portion of the longwave emission spectrum would uncover novel information about water vapor in clear skies and optically thin clouds, including polar stratospheric clouds. Polar stratospheric clouds, which occur most frequently over the Antarctic Plateau, are of particular interest in the far-infrared as they are always very thin, high-level ice clouds. The mid-infrared portion of the spectrum does not hold as much information about water vapor that the far-infrared has, but it still houses the transparent and semi-transparent spectral windows, which can help characterize surface temperatures in clear-sky conditions. Being able to model water vapor using

far-infrared measurements plays a key role on both local and global energy scales. This ties into the spectral greenhouse effect, where Earth absorbs and retains solar radiation through various atmospheric constituents, including water vapor, ultimately reducing radiative cooling to space. Since measurements in far-infrared areas of the longwave spectrum have been limited, we do not have a full picture of how water vapor presence impacts the emission spectrum.

Past attempts to resolve the far-infrared spectrum relied on long integration times and were short-lived experiments (L'Ecuyer et al. 2021). For example, the Nimbus-3 and Nimbus-4 contained Infrared Interferometer Spectrometer (IRIS)-B and IRIS-D instruments to measure the far-infrared spectrum up to 25 μm (Conrath et al. 1970; Hanel et al. 1970). The last satellite-based experiment that measured far-infrared wavelengths was more than four decades ago during the Russian Meteor-28 and Meteor-29 satellites in the 1970s, and all missions afterward were only broadband measurements with no spectral resolution (Spankuch and Dohler, 1985; Timofeev et al. 2019; L'Ecuyer et al. 2021). Having spectrally resolved measurements of far-infrared wavelengths is important to be able to fully characterize a vertical atmospheric profile. While there have been spectrally resolved measurements in the thermal infrared by satellite instruments – for example: the Atmospheric Infrared Sounder (AIRS), the Infrared Atmospheric Sounding Interferometer (IASI), MODIS, and others – these instruments only measure into the mid-infrared range.

The consequences of this lack of far-infrared measurements translates to more than half of outgoing longwave energy having not been measured (Huang et al. 2014). Accurate models of water vapor, surface emissivity, and cloud properties rely on complete spectral measurements in the far-infrared. It is expected that polar surfaces, especially in drier areas, will experience a variety of different emissivities at different far-infrared wavelengths (Huang et al. 2016). In cloudy

conditions, the scattering properties of ice particles will have an impact on the far-infrared spectral measurements (Chen 2020). Surface emissivity, water vapor presence, and cloud presence – especially optically thin, high clouds (Harries et al. 2008) – will be crucial in understanding polar energy imbalances. Furthermore, we can better understand Arctic warming, the rate of ice melt, and global energy balance with more accurate far-infrared measurements (L'Ecuyer et al. 2023).

Since there has been recognition of the importance of spectrally resolved far-infrared measurements, there have been three missions developed by the National Aeronautics and Space Administration (NASA), the European Space Agency (ESA), and the Canadian Space Agency to help fill this gap in measurements. The three missions are: the Polar Radiant Energy in the Far Infrared Experiment (PREFIRE), the Far Infrared Outgoing Radiation Understanding and Monitoring (FORUM) mission, and the Thin Ice Clouds in the Far Infrared Experiment (TICFIRE) (Libois et al. 2015; Palchetti et al. 2020; L'Ecuyer et al. 2021). This study will focus on the PREFIRE mission.

1.3 PREFIRE

NASA and ESA recognized the importance of having a full picture of far-infrared measurements and chose two satellite missions to fill this gap in measurements: the FORUM mission, launching in 2026, and the complementary PREFIRE mission, launching in 2024.

The PREFIRE mission, launching first, is a low-cost, mid-spectral resolution satellite mission that will consist of two 6U CubeSats taking measurements between 5 and 55 μm on subdaily and seasonal timescales. The two CubeSats will be in separate polar orbits, measuring far-infrared data on a global scale but with many of the CubeSat intersections occurring over high-latitude regions. The range of outgoing longwave radiation (OLR) measurements on PREFIRE

will include over 95% of Earth's OLR (L'Ecuyer et al. 2021). The PREFIRE CubeSats will be able to gather a lot of information from the relatively transparent, dry, high-latitude atmospheres. Surface ice sheet temperatures, ice sheet mass balance and ice melt, thermodynamics, surface emissivity, and top-of-atmosphere far-infrared spectra of polar regions will be monitored and assessed.

Each CubeSat will have 8-point spectrometers operated by a push broom scanner, meaning the line of measurements will be perpendicular to the direction of CubeSat flight. The spectrometers are referred to as thermal infrared sensors (TIRS). The satellites are anticipated to have altitude ranges of 250-530 km and orbit inclinations between 70° and 98°, though the specifics will not be known until the specific launch date is selected (L'Ecuyer et al. 2021). The TIRS measurements on each CubeSat will be measuring in the mid- and far-infrared spectrum between 5 and 55 μm at a resolution of 0.86-μm for a total of 54 unique measurements per pixel, as there will be channel gaps at 7, 15, and 30 μm due to instrument constraints. Each of the 8 pixels will cover a 10 km by 10 km region with 20 km in between the pixels. The TIRS are calibrated at least eight times per orbit by rotation of a calibration mirror, and comparison between other satellites and ground-based observations will contribute to additional calibration in-flight. (L'Ecuyer et al. 2021).

The PREFIRE satellite mission will serve as a valuable tool for understanding radiative properties and energy balance dynamics in polar regions. Before PREFIRE is launched, TIRS measurements are simulated over specific polar locations where there are surface observations. The two data sources used for polar surface observations are the Antarctic Meteorological Research and Data Center (AMRDC) and the Integrated Characterization of Energy, Clouds, Atmospheric state, and Precipitation at Summit (ICECAPS) project.

1.4 AMRDC AWS Network

Polar regions experience extreme weather events that are difficult to fully describe since the climate is very harsh, limiting human activity and thus in-situ observations. While satellite observations are useful for observing these regions, there was still a need for surface meteorology observations. This is why the development of automatic weather stations (AWS) was necessary to be able to observe these extremely cold climates without needing to have a constant human presence.

The prototype AWS – named Stanford AWS – was developed and deployed in 1975 by Stanford University's Center for Radio Astronomy. This Stanford AWS began taking measurements of temperature, air pressure, wind speed and direction at the South Pole. It was then moved to McMurdo and finally to Marble Point. This prototype transmitted its data to the polar-orbiting Nimbus-6 satellite and operated until 1977. After its success in obtaining data in the Antarctic, the National Science Foundation (NSF) funded six more Antarctic AWS which operated during 1978-79 in the McMurdo and Byrd area. In 1978, the Argos satellite system was developed, and the AWS were redesigned to transmit surface meteorological data every 200 s via Argos (Lazzara et al. 2012).

The University of Wisconsin-Madison's (UW-Madison's) AMRDC took over the U.S. Antarctic Program (USAP) AWS program in 1980. By 1982, there were 13 AWS installed in Antarctica. Most of the stations were deployed at easier-to-access, low-elevation, coastal locations (with the exception of the high polar plateau station Dome C). In the 1990s, the AMRDC collaborated with the British, French, Italian, and Japanese Antarctic programs, where they all recognized the need to install more AWS in all parts of the continent, including more difficult-to-

access high polar plateau regions. Further AWS were installed to monitor intense katabatic wind events (Lazzara et al. 2012).

Katabatic wind events occur due to radiative cooling in high-elevation regions of the Antarctic and Greenland ice sheets in their respective winters when there is little to no solar radiation. When there is this net radiation loss high on the ice sheet, a pool of cold air is formed, the air density increases and airflow begins downslope, warming adiabatically and reaching very high speeds. In Antarctica, katabatic winds originate from either the East or West Antarctic Plateau, with the majority of originating on the East Antarctic Plateau (Turner 2015). The winds then rush down at high speed to lower-elevation coastal regions and valleys, helping in the process of cyclogenesis due to their relatively cold air meeting and mixing with off-continent, relatively warmer maritime air (Turner 2015). Polar winds also affect how snow moves and accumulates. Snow is frequently transported from higher areas on the Antarctic Plateau to lower elevations by high winds before being permanently added to the underlying snow cover at the lower elevation areas (Groot et al. 2013). On average, it takes a constant wind speed of about 4 m/s to add snow to the underlying snow cover, although lower wind speeds can still contribute to the underlying snow. High wind speeds especially contribute to snow types becoming more spherical and less dendritic, causing their emissivity to change, which can impact satellite readings over the affected areas (Groot et al. 2013). The AMRDC has recognized the importance of having AWS in locations prone to experiencing katabatic wind events.

In the 1990s, the AWS network expanded to encompass katabatic wind research projects. AWS were installed around Reeves Glacier and the Adélie Land coast at Cape Denison and Port Martin (Lazzara et al. 2012). The anemometers were updated throughout this decade until they were able to withstand the high katabatic wind speeds. Other sensors were updated in the 2000s to

be able to withstand the harshest, coldest conditions on the polar plateau. AWS were also updated so that they were not only transmitting to the Argos satellite system but to Iridium systems as well.

The AWS transmit data to the AMRDC at UW-Madison via these two satellite systems. The data is acquired within 24 hours and quality controlled within one month. With over 120 AWS internationally, the AMRDC accounts for over half of all operational AWS in Antarctica (Bumbaco et al. 2012). This can be visualized in Figure 1.1 which shows all of the international AWS on the left compared to the AMRDC's AWS on the right.

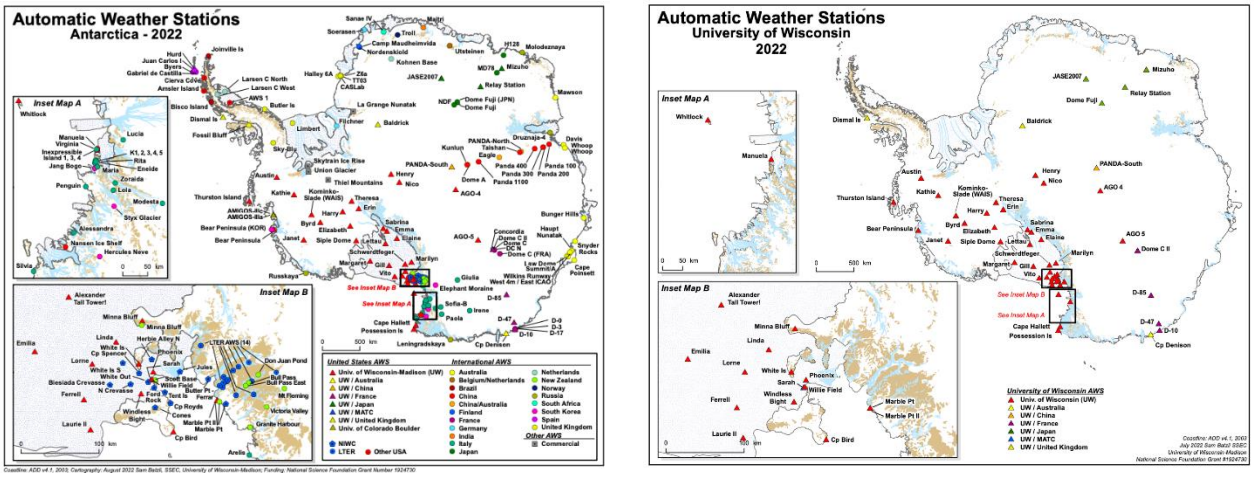

Figure 1.1: Location of all international AWS (left) and AWS associated with UW-Madison's AMRDC (right) as of 2022 (AMRDC 2022).

AWS data has also been used in the past to validate satellite data from various missions. For example, the study by Picard et al. 2013 used AWS to validate ground-based radiometric measurements around Dome C AWS. Another study done by Scambos et al. 2018 used AWS to validate the Moderate Resolution Imaging Spectroradiometer (MODIS) Terra and Aqua measurements of extreme cold temperatures on the East Antarctic Plateau.

The AMRDC has recognized the importance of having a vast network of AWS in Antarctica in order to characterize record low temperatures, katabatic winds, surface melt, validation of satellite data, and other meteorological events. Two of the AWS locations from the

AMRDC that will be focused on in this thesis are the coastal station, Dismal Island (68.088 °S, 68.826 °W) and the inland station, Dome C II (75.106 °S, 123.347 °E).

In the Arctic, there is a complementary network of observations, and this paper will be focusing on the ICECAPS project in Greenland.

1.5 ICECAPS

In the Arctic, surface measurements are made on the Greenland Ice Sheet through the ICECAPS project. This project, located on the summit of the ice sheet (72° 36'N, 38° 25'W), is a collaborative project between the University of Colorado, Washington State University, Vanderbilt University, University of Oklahoma, and UW-Madison. There were previously measurements made on Greenland's summit through the AMRDC with a network of 8 AWS, but these stations were decommissioned in the 1990s. The research station, Summit Station, was established in 1989 with continuous annual staff since 2003. In 2010, the ICECAPS project was created which substantially improved the way surface meteorology, cloud, atmosphere, and precipitation properties were measured (NOAA n.d.). The location of Summit Station, as well as other major Arctic surface observation locations, are shown in Figure 1.2. However, this does not show an exhaustive list of all Arctic observation stations. The ICECAPS project is used to simulate PREFIRE measurements over Summit Station, Greenland for this thesis project.

Figure 1.2: Location of some major research stations in the Arctic, including Summit Station located on Greenland's Summit (Ahlenius 2008).

1.6 Simulations of PREFIRE TIRS using polar surface observations

This thesis project will simulate the PREFIRE TIRS measurements on annual and seasonal timescales at three specific locations that have surface observations: Dismal Island AWS (located on the Antarctic coast), Dome C II AWS (located on the Antarctic plateau), and Summit Station (located on the Greenland summit). The model used to simulate the TIRS is the principal component-based radiative transfer model (PCRTM), which outputs high-spectral resolution data. Spectral response functions (SRFs) are then used to convolve the high-spectral output to the PREFIRE-specific TIRS measurements. Various weather conditions are simulated at each location in order to predict how sensitive the TIRS will be in three distinct polar regions.

General and unique weather conditions including the annual cycle, surface melt events, katabatic wind events, inversion presence, water vapor concentration, and various levels of cloud presence are simulated and analyzed to determine TIRS sensitivity. The annual cycle is simulated first, where a comparison is made between the surface temperature, the high-spectral PCRTM

output, and the convolved TIRS output. The sensitivity of TIRS is discussed by analyzing its timeseries at each location and understanding the role of inversions. Next, surface type (and thus surface emissivity) changes are simulated at each location. At Dismal Island, a surface freeze event is simulated by analyzing the difference between a water surface and an ice surface. At Summit Station, a surface melt event is simulated by analyzing the difference between a fine snow surface and a water surface. At Dome C II, a katabatic wind event is simulated by analyzing the difference between larger, dendritic snow and smaller, finer snow. All of these simulations are done with a clear-sky atmosphere, and cloud presence at various levels in the atmosphere is simulated next.

When simulating cloud presence, the sensitivity of TIRS to cloud presence and cloud phases are explored first. At Dome C II, cloud presence is analyzed against a clear sky atmosphere. At Dismal Island and Summit Station, cloud phases are analyzed. This includes comparing mixed-phase clouds against ice clouds, and liquid clouds against ice clouds. Then, three types of clouds are analyzed at each location: low-level clouds, mid-level clouds, and high-level clouds. The clouds are either ice, mixed-phase, or liquid depending on the location. At Dome C II, all clouds simulated are ice, and the low-level clouds simulated are representative of diamond dust, and the high-level clouds simulated are representative of polar stratospheric clouds.

The goal of this thesis is to understand the range and magnitude of what the PREFIRE TIRS will measure over specific polar regions where there are surface observations during a variety of unique weather conditions.

2 Data and Methods

2.1 PCRTM

Developed by Liu et al. 2006, the forward principal component-based radiative transfer model (PCRTM) is used in this paper to simulate high-spectral resolution, infrared satellite data by predicting the principal component (PC) scores of the channel radiance and transmittance spectra given specific inputs. This model is run in Python using the pyPCRTM package created by UW-Madison researcher Aronne Merrelli with specifications to simulate the PREFIRE TIRS signatures.

There are computational requirements and challenges involved in analyzing data from modern remote sensing instruments with high-spectral and spatial resolution. The radiative transfer forward model plays a key role in relating atmospheric profiles to observed radiances, but this model can be computationally expensive due to the large number of calculations needed for high-resolution data. Instead of doing these computationally expensive line-by-line calculations, PCRTM recognizes that there are redundancies in many radiative transfer calculations, as many infrared regions contain similar information in terms of Lorentz or Doppler half-widths. Line intensity and half-width dependencies on temperature and pressure are similar, so the number of unique pieces of information is less than the number of monochromatic radiances. Thus, PCRTM removes these redundancies and predicts the PC scores of the channel radiances and transmittances and compresses the abundance of information found in high-resolution infrared spectra, saving a lot of computational time but preserving accuracy of the far-infrared spectrum. This model has been used successfully for the NPOESS airborne sounder tested interferometer (NAST-I)

instruments, AIRS instruments (Liu et al. 2006), the IASI satellite sensor (Liu et al. 2009), and the PREFIRE TIRS instruments (Miller et al. 2023).

The model used to train PCRTM is a Line-By-Line Radiative Transfer Model (LBLRTM) (Liu et al. 2009). In the Liu et al. 2009 study, the outputs for PCRTM and LBLRTM have a root mean square error (RMSE) of less than 0.05 K and bias errors of less than 002 K. This study uses IASI data for the model output comparisons, which is a satellite sensor that measures in the infrared spectrum from 3.6 to 15.5 μm. Since IASI does not span the entirety of PREFIRE's spectral range, the output data is instead used from the Climate Absolute Radiance and Refractivity Observatory (CLARREO) mission. CLARREO contains infrared data from 3.6 to 200 μm, which includes the range of wavelengths that PREFIRE will measure. Considering the RMSE of less than 0.05 K between PCRTM and LBLRTM for the IASI sensor, we have confidence that PCRTM is accurate using CLARREO data to simulate PREFIRE measurements.

The PCRTM model works by generating a set of orthogonal eigenvectors (PCs) by decomposing a data matrix of channel radiances using singular value decomposition (SVD). The PCs capture the spectral variations of top-of-atmosphere (TOA) radiances between different channels, while the associated PC scores capture the dependencies of the infrared spectra on atmospheric temperature and constituent profiles. The PC scores can then be predicted by linearly combining a subset of significant PCs and projecting channel radiances onto them. PCRTM also reduces computational time by avoiding redundancies, so fewer predictors are needed for prediction. PCRTM can interpret results in the PC domain and spectral domain in order to interpret atmospheric profiles. In this paper, the model's inputs are specified to simulate PREFIRE measurements.

The inputs to PCRTM are set on 101 fixed vertical pressure levels. Inputs include vertical profiles of temperature, specific humidity, ozone, carbon dioxide, methane, carbon monoxide, and nitrous oxide, surface temperature, pressure, and emissivity, TOA (observer) pressure, and sensor zenith angle. The last two are fixed values that are specified at 0.005 hPa and 0.0 degrees. Clouds can also be added to the model by specifying their pressure level, type (ice or liquid), effective radius, and optical depth. Clouds are simulated in PCRTM by using pre-computed transmittances and reflectances. Calculations are then made for their single and multiple scattering properties using complex indices of refraction in the far-infrared, based on the specific cloud input (Liu et al. 2006; Liu et al. 2009).

The general PCRTM output models a thermal infrared spectrometer instrument that covers a continuous spectral range of wavelengths from 50 to 2760 cm^{-1} (approximately 3.6 to 200.0 μm) with a wavenumber sampling interval of 0.5 cm^{-1}. This high-spectral output is then convolved to the PREFIRE-specific TIRS measurements using spectral response functions (SRFs).

2.1.1 Convolving TIRS using SRFs

PCRTM's general output is a high-resolution spectrum that contains detailed information about radiances and transmittances at various wavelengths. Though the model contains high-spectral information for wavelengths between 3.6 to 200.0 μm, the TIRS instruments will not be obtaining information for wavelengths longer than 55 μm, so the wavelengths beyond 55 μm from the PCRTM output are ignored. The PCRTM output is shown in Figure 2.1a in terms of radiances, however, this thesis project will be converting the radiances to brightness temperatures for all simulations. In order to convert the general high-spectral output to PREFIRE-specific measurements, the radiances are converted to simulated TIRS measurements using SRFs.

SRFs describe the sensitivity of the TIRS instrument at different wavelengths by specifying how the instrument's response varies with respect to incoming radiation at different frequencies. There is a unique SRF for each of the 54 TIRS channels, however, there will be gaps in measurements at 7, 15, and 30 μm due to constraints caused by the edges of the filters on the TIRS instruments. Each unique SRF for the 54 channels is shown in Figure 2.1b. The high-spectral PCRTM outputs are then convolved with SRFs to simulate the response of the TIRS instrument.

The TIRS radiances after convolution with SRFs are shown in Figure 2.1c. Although there may be fewer channels than 54 once the PREFIRE CubeSats are in operation, this analysis assumes that all 54 channels are useable.

This process using SRFs effectively integrates the spectral information over the TIRS sensitivity range. Figure 2.1, which was produced in the Miller et al. 2023 study, shows how the high-spectral output (Figure 2.1a) is convolved to the PREFIRE TIRS (Figure 2.1b) using SRFs (Figure 2.1c), as well as information about the instrument's noise: noise equivalent delta radiance (NEDR, Figure 2.1d) and signal-to-noise ratio (SNR, Figure 2.1e).

The NEDR provides an estimate of the sensitivity for each of the 54 PREFIRE TIRS channels, quantifying the minimum detectable change in radiance that the instrument can distinguish from background noise. The SNR is defined by the ratio of the radiance to the NEDR, and it indicates the level of the signal compared to the background noise. Higher SNR ratios indicate a stronger and more distinguishable signal relative to the noise, which occurs within the wavelength range of 8-28 μm. Lower SNR ratios indicate a weaker signal compared to the noise, which occurs at wavelengths larger than 30 μm. It is expected that PREFIRE will be able to resolve brightness temperature retrievals within approximately 1 K for one specific scene. With more measurements of many different scenes, the error in retrieval will be reduced by the square root of

the number of samples, and the minimum detectable change in brightness temperature will become lower than the single-scene threshold of 1 K.

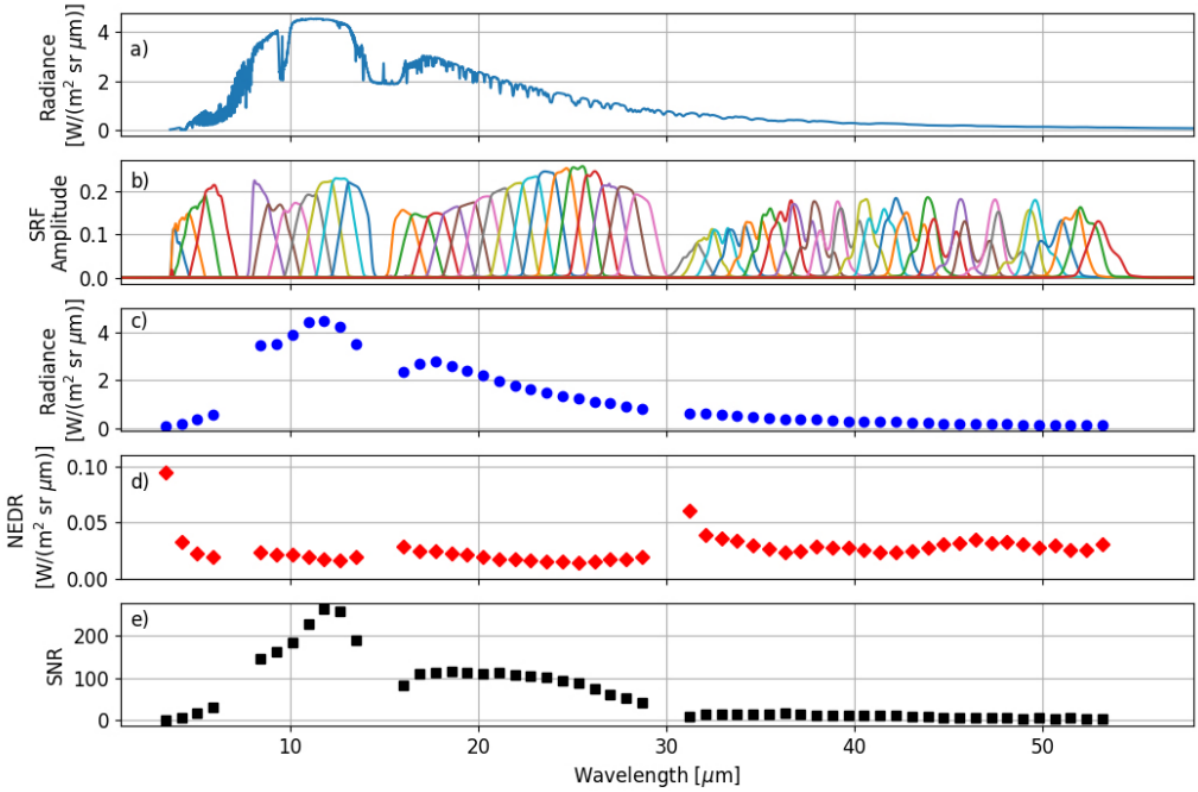

Figure 2.1: a) PCRTM high-spectral output using a sub-Arctic winter profile (McClatchey et al. 1972), b) PREFIRE-specific modeled SRFS for the 54 channels, c) TIRS radiances after high-spectral resolution in a) is convolved with the SRFs from b), d) Noise-equivalent delta radiance (NEDR), and e) the signal-to-noise ratio (Miller et al. 2023).

Since there is not yet real PREFIRE data, the data is simulated in this paper at specific locations where there are surface observations.

2.2 Data input sources

The three locations chosen to simulate PREFIRE data are Dome C II (75.106° S, 123.347° E), Dismal Island (68.088° S, 68.826 ° W), and Summit Station (72.60 ° N, 38.42 ° W). The first

two stations, located in Antarctica, will source data from the AMRDC while the last station, located in Greenland, will source data from ICECAPS. PREFIRE data is simulated for the year 2012 since there was a significant surface melt event that occurred in Greenland during the year's summer (Hall et al. 2013). This year was also a time period where AWS exhibited minimal measurement errors, yielding a substantial amount of useful surface observation data.

2.2.1 AMRDC data

The two locations chosen to simulate PREFIRE data over Antarctica are located on the Antarctic Peninsula (Dismal Island) and the Antarctic Plateau (Dome C II). There are significant climatic and elevation differences between these two locations, making them interesting case studies to simulate PREFIRE data. Dismal Island exists at 12 m above sea level whereas Dome C II is at 3250 m. Dismal Island captures the influences of maritime air masses and interactions with the Southern Ocean, experiencing warmer temperatures and a greater potential for moisture. Dome C II represents an extreme inland Antarctic climate, characterized by frigid temperatures, a dry atmosphere, and stable atmospheric conditions, making it prone to strong inversions, especially in the austral winter. By using the data from these contrasting locations, the PREFIRE simulations can capture differences in coastal versus inland Antarctic atmospheric conditions.

The data used for each of these locations are the surface temperature and surface pressure as input to PCRTM. In the case that the sensors have erroneous data, the data is replaced with surface data from the European Centre for Medium-Range Weather Forecasts (ECMWF) Reanalysis v5 (ERA5).

Example AWS data is plotted in Figure 2.2 with Dismal Island on the left and Dome C II on the right. The red line is the temperature timeseries from January 2012, which is capturing the

austral summer and diurnal cycle, and the blue line is the temperature time series from July 2012, which is capturing the austral winter and the effects of synoptic storms with a lack of diurnal cycle.

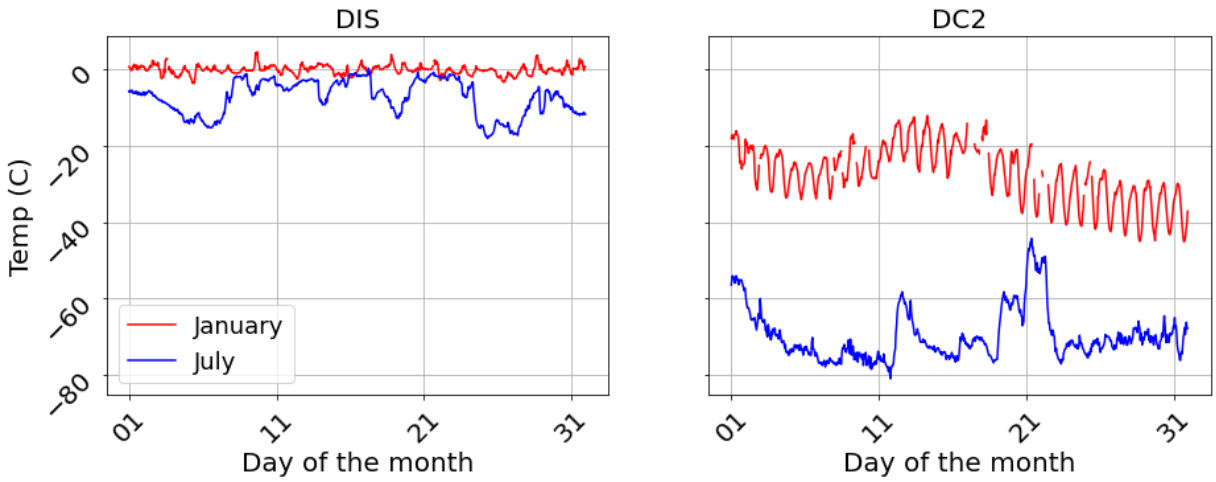

Figure 2.2: Dismal Island (DIS) (left) and Dome C II (DC2) (right) temperature timeseries for the months of January (red) 2012 and July (blue) 2012.

2.2.2 ICECAPS data

The location chosen to simulate PREFIRE data over the Arctic is located in Greenland on the Summit (Summit Station). This station has a similar elevation to Dome C II, sitting at 3200 m above sea level. Summit Station complements the Antarctic stations by providing its own distinct climatic and environmental characteristics. By incorporating Summit Station data into PREFIRE simulations, unique Arctic dynamics and processes can be studied, such as the Greenland surface melt event. By comparing data from both polar regions, patterns and anomalies can be compared and analyzed.

Similarly to the AMRDC data, the data used from ICECAPS includes surface temperature and surface pressure. Surface data from ERA5 is used here as well in the case of erroneous data.

Example data from ICECAPS is plotted in Figure 2.3, where the red line is the 2012 July temperature timeseries and the blue line is the 2012 January temperature timeseries.

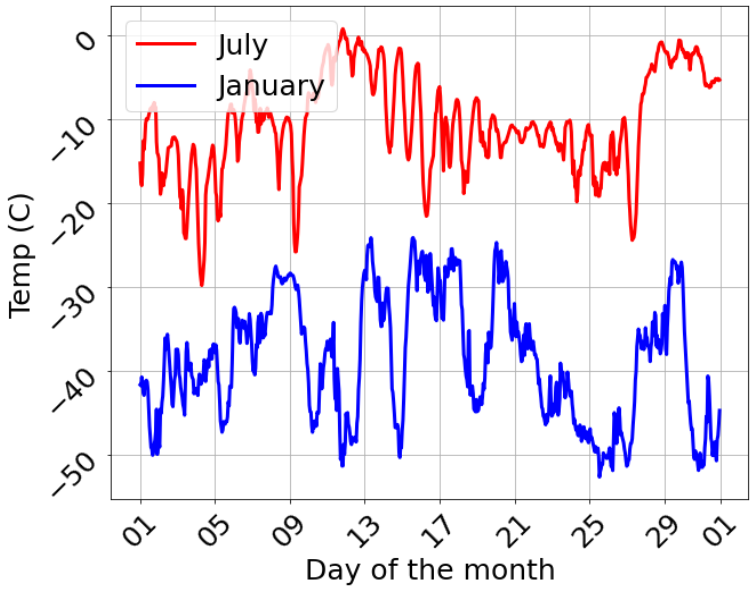

Figure 2.3: Summit Station temperature timeseries for the months of July (red) and January (blue) 2012.

2.2.3 ECMWF and standard atmospheric profile interpolation

ERA5 data, obtained from ECMWF, plays a vital role in the simulation of PREFIRE data. ERA5 data provides a comprehensive set of atmospheric information, including vertical profiles of temperature, pressure, humidity, and various constituents such as carbon dioxide, carbon monoxide, nitrous oxide, methane, and ozone. The ERA5 data used is given on 37 unique pressure levels (Hersbach et al. 2020).

As stated in section 2.1, PCRTM needs an input that is on 101 unique vertical pressure levels. To bridge the discrepancy between the 37 vertical pressure levels provided by ECMWF and the 101 vertical pressure values required by the PCRTM model, an interpolation process was employed in this study. A widely accepted standard atmospheric profile based on the work of

McClatchey et al. 1972 was utilized. This study provides a standard polar atmospheric profile based on summer or winter environments, and it includes a comprehensive set of vertical profiles for atmospheric parameters including temperature, pressure, and the various atmospheric constituents that contribute to the greenhouse effect. This study uses carbon monoxide and nitrous oxide values as inputs to PCRTM, and these values are specified in McClatchey et al. 1972 based on either a sub-Arctic winter or summer. Fixed values of carbon dioxide (400 ppm) and methane (1.8 ppm) are also used as inputs.

Since PCRTM runs on 101 fixed pressure levels in its input, the ERA5 data is interpolated with the standard atmospheric profiles. The interpolation involves mapping the ERA5 data onto the vertical pressure grid of the standard atmospheric polar profile, which also includes interpolating the TOA values of temperature, humidity, and ozone since ERA5 does not have an accurate resolution of these TOA values. This interpolation process allows for the integration of ERA5 data with PCRTM model input necessities, enabling accurate simulations and analysis based on a more extensive set of vertical pressure values.

An example output is shown in Figure 2.4, where the important window and absorption locations in the mid- and far-infrared are also identified. There are many strong absorption bands of water vapor throughout the mid-infrared region between 3 and 7 μm. At 9.6 μm, there is the ozone absorption band. The transparent window, which can see through to the surface in the absence of clouds, occurs between 11 and 12 μm. The carbon dioxide band occurs strongly at 15 μm. There is then the partially transparent window that occurs between 18 to 25 μm. The brightness temperatures are warmer in this range when it is less influenced by water vapor absorption, and they are colder when it is more influenced by water vapor absorption due to the differences in the amount of radiation that reaches the satellite. Beyond 25 μm, the atmosphere is virtually opaque

and very sensitive to even the smallest amounts of water vapor. The purple vertical dotted line shows where there have not been spectrally resolved measurements before, where PREFIRE will be making novel measurements.

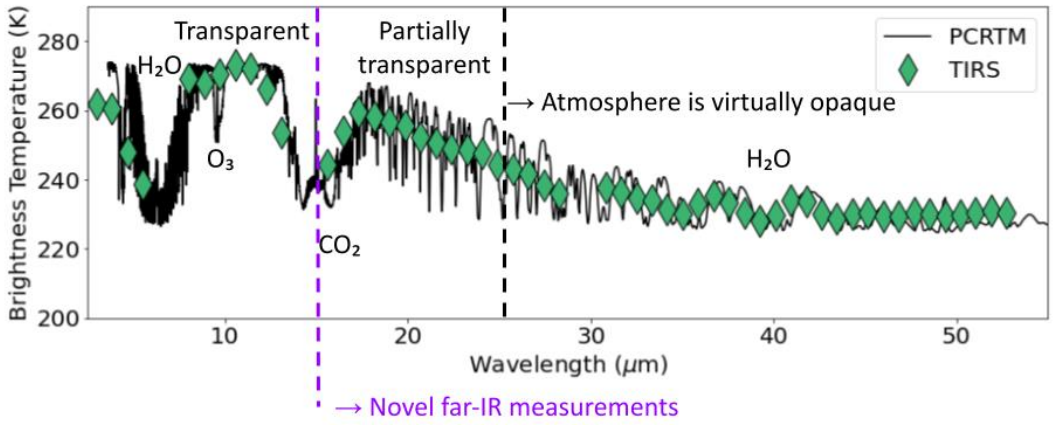

Figure 2.4: Example high-spectral PCRTM output (solid black line) and PREFIRE-specific TIRS (green diamonds) spectral responses for Dismal Island in the austral summer. Key transparent windows and absorption locations are labeled. The vertical purple dotted line indicates the beginning of the novel far-infrared measurements PREFIRE will be resolving, and the vertical black dotted line indicates where the atmosphere is virtually opaque.

2.2.4 Emissivity dataset

To obtain accurate surface emissivity values for the three locations, this study relies on the comprehensive surface emissivity dataset for the far-infrared developed in the Huang et al. 2016 study. The emissivities are calculated for the entire longwave spectrum using radiative transfer techniques and index of refraction measurements, and then they are regressed using MODIS retrievals of surface emissivity. The data is then compared against surface emissivity retrievals from IASI measurements, which showed favorable agreement in the mid-infrared spectrum. Considering this favorable agreement in the mid-infrared, there is confidence that the far-infrared

surface emissivities are accurate, though this cannot be completely validated until after PREFIRE launches and there exists far-infrared satellite observations.

The dataset has five distinct surface types: fine snow, medium snow, coarse snow, ice, and water, which serve as potential inputs to PCRTM. In this thesis, all surfaces except for medium snow are employed for the simulations, and a discussion on the surface simulation methods will be presented in section 2.3.2. Figure 2.5 shows the four different types simulated in this study and their emissivity values that are used as PCRTM input. The plot shows only the surface emissivity values in the PREFIRE range, which excludes wavelengths longer than 55 μm.

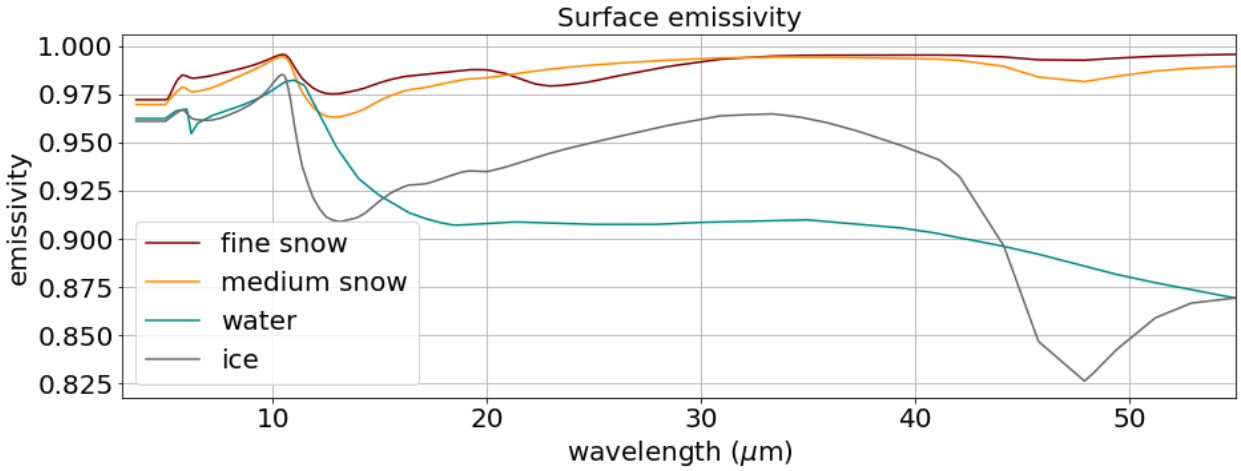

Figure 2.5: Values of surface emissivity for four different surface types: fine snow (red), medium snow (orange), water (green), and ice (gray) based on the Huang et al. 2016 study.

2.3 Methods

The simulations at the three locations involve using the ERA5 data, which has a grid box resolution of 0.25° by 0.25°. The data was matched to the nearest degree of latitude and longitude for each location, resulting in Dismal Island being simulated at 68.00 °S; 68.75 °W, Dome C II at 75.00 °S; 123.25 °E, and Summit Station at 72.50 °N; 38.50 °W. This study is organized by three

main simulations: the annual cycle, surface emissivity, and cloud sensitivity. The following sections describe the specific methods by which these topics are simulated.

2.3.1 Annual cycle simulations

In order to gain an insight into the variability we can expect at the surface and thus in the transparent and semi-transparent window channels of the TIRS, a temperature timeseries is generated from the observational data and discussed for the year 2012 at each of the three locations. Then, to simulate the general annual TIRS outputs, PCRTM was run every 12 hours throughout the year of 2012 for each of the three locations, allowing for enough temporal resolution to capture the diurnal cycle and potential variations in atmospheric conditions. The PREFIRE CubeSats will intersect each other's orbit (or their own orbit), ranging anywhere from 30-minute intervals to 24-hour intervals in a day, so the 12-hour temporal resolution was chosen to provide sufficient temporal detail while minimizing computational time. The total simulated scenes for each station for the year 2012 is 732. The simulated TIRS data is then plotted against the high-spectral PCRTM outputs to compare the range of brightness temperatures captured by each. The TIRS data is then plotted against itself at different wavelengths for each location and organized by season to gain insight into the differing outputs on an annual timescale.

The TIRS outputs are then analyzed further to assess the occurrence of inversions – when the temperature increases with height instead of decreases – with the use of weighting functions. The patterns of inversions and their frequency are identified, providing insight into the atmospheric stability at each location throughout the year and how sensitive TIRS will be to inversions.

Three specific TIRS channels were selected for further analysis: the 11.4-μm transparent window channel, the 22.4-μm partially transparent (or "dirty") window channel, and the 35.0-μm

water vapor channel. A timeseries is created for each of these three channels at each of the three locations, and an analysis is done on how these channels evolve over time, giving insight to the annual variability we can expect from the TIRS measurements.

2.3.2 Surface emissivity simulations

Three surface emissivity simulations are done in this study: a surface freeze event, a surface melt event, and a wind event affecting snow grain size. For all studies, simulations are conducted by altering only the surface type while keeping all other PCRTM inputs unchanged. Then, the difference is taken between the two outputs in each simulation in order to determine the TIRS sensitivity to unique surface types.

For the surface freeze event, the study is done at Dismal Island, where the temperature reaches above 0°C more frequently than the other locations. The date and time chosen for the freeze event is September 1, 2012 at 08 Z, selected based on the temperature trend transitioning from above freezing to below freezing around this time, providing suitable conditions for a surface freeze event. The two surface types simulated on this date are a water surface and an ice surface.

For the surface melt event, the study is done at Summit Station, where there was an extensive surface melt event on the Greenland ice sheet during July 2012 (Hall et al. 2013). The date chosen for the melt event is July 11, 2012 at 16 Z, selected to be consistent with the melt dates identified in the Hall et al. 2013 study. The two surface types simulated on this date are a fine snow surface and a water surface.

For the wind event, the study is done at Dome C II, a location that is impacted by katabatic winds originating on the East Antarctic Plateau. Based on the study done by Groot et al. 2013, winds exceeding 4 m/s can affect the dendricity and sphericity of surface snow grain, causing them

to become less dendritic and more spherical with higher wind speeds. According to the American Meteorology Society, the definition for katabatic wind ranges from 3 to 8 m s^{-1} for mountain-valley wind systems where polar regions can have katabatic winds that reach up to 50 m s^{-1}. The date chosen to simulate a katabatic wind event is May 9, 2012 at 10Z. At this time, wind speeds were nearly 10 m s^{-1}. The two surface types simulated on this date are a medium snow surface and a fine snow surface.

2.3.3 Cloud sensitivity simulations

The final section of the results for this thesis project is the TIRS sensitivity to cloud simulations. Cloud presence versus clear sky and cloud phases are simulated first. Then, at each location, low-level clouds, mid-level clouds, and high-level clouds are simulated. The clouds are set in the atmosphere based on the most probable effective radius and optical depth (OD) presented in past polar cloud studies (Stone 1993; Mahesh 2001; Lachlan-Cope 2010; Petterson et al. 2018; Lacour et al. 2019). The height of clouds is set by calculating the pressure level of the cloud using the hypsometric equation:

$$\Delta Z = \frac{R\bar{T}_v}{g} \ln\left(\frac{P_1}{P_2}\right) \quad (1)$$

where P2 is the pressure level calculated as the cloud input to PCRTM, P1 is the surface pressure specific to the location, date, and time, ΔZ is the height of the cloud measured from the surface, R is the specific gas constant for dry air (287.047 J kg^{-1} K^{-1}), g is the gravitational constant 9.81 m s^{-1}, and $\overline{T_v}$, the mean virtual temperature, is calculated as:

$$\overline{T_v} = \bar{T}(1 + 0.61\bar{q}) \quad (2)$$

where $\bar{T}$ and $\bar{q}$ are the mean temperature in Kelvin and mean specific humidity in kg/kg in the low-, mid-, or high-level atmosphere based on the PCRTM input soundings at each specific location and time.

In this section, the cloud simulation methods are presented for each location. All clouds are simulated on January 1, 2012 at 00 Z, apart from Dismal Island which includes the exact same cloud simulations done six months later on July 1, 2012 at 00 Z. The goal is then to analyze the TIRS outputs to determine their sensitivity to different level clouds with various effective radii and ODs.

The methods for cloud simulations of Dismal Island will be discussed first. Based on the studies done by Mahesh 2001 and Lachlan-Cope 2010, effective radii of clouds on the Antarctic Peninsula range from 5 to 25 μm and ODs are generally greater than 10. The types of clouds can be liquid, mixed-phase, or ice, with fully ice clouds occurring most often when temperatures are less than -30 °C. When simulating low-level clouds at Dismal Island, the clouds are set as liquid clouds 1 km above the surface. Mid-level clouds are set as liquid clouds 5 km above the surface, and high-level clouds are set as ice clouds 10 km above the surface. For each level, all PCRTM inputs are kept constant except for the effective radius, which is changed between 5, 15, and 25 μm. Then, the OD is changed between 10 and 30 while everything else is kept constant. The simulations are done for January 1, 2012 at 00 Z and again for July 1, 2012 at 00 Z. For Dome C II and Summit Station, only January 1, 2012 at 00 Z is used as a simulation time.

For cloud simulations done at Summit Station, the effective radii and OD estimations are used from the studies done by Petterson et al. 2018 and Lacour et al. 2019. These studies conclude that effective radii of inland Greenland clouds range from 5 to 30 μm and ODs range from 1 to 15. Similarly to Dismal Island, fully ice clouds tend to form when temperatures are less than -30 °C.

At temperatures higher than this, mixed-phase clouds are likely to form in Greenland. Low-, mid-, and high-level clouds are set at 1, 5, and 10 km respectively – the same as Dismal Island. At each level, the effective radius is changed between 5, 15, and 25 μm, and then the OD is changed between 1 and 15.

Finally, for cloud simulations done at Dome C II, the cloud estimations of effective radii and OD are approximated using results from the Stone 1993, Mahesh 2001, and Lachlan-Cope 2010 studies. Effective radii estimates have a high range between 5 and 1000 μm, where those higher values are essentially snowflakes, and OD estimates are generally less than or equal to 1. All clouds at this location are ice clouds. Low-level clouds simulated at this location are diamond dust, which is a surface-level cloud that is composed of ice crystals. The level that the diamond dust is set at is 0.25 km above the surface, and then the effective radius is changed between 2, 12, and 1000 μm to simulate very small particles, the average effective radius of diamond dust, and larger near-surface snowflakes. The OD is changed between 0.1 and 1. When simulating mid-level ice clouds, the clouds are set at 5 km and the effective radius is changed between 5, 30, and 50 μm. The OD is changed between 0.5 and 1. For high-level clouds at Dome C II, polar stratospheric clouds (PSCs) are simulated. These clouds occur very high in the atmosphere, so this study sets them at 25 km. The effective radius is changed between 1 and 10 and the OD is changed between 0.1 and 1.

For all simulations, the goal is to determine how sensitive the PREFIRE TIRS will be to different atmospheric and surface conditions.

3 Results

3.1 Annual cycle

The PREFIRE mission lifetime will be between 1 to 2 years, so in order to gain insight into how the TIRS brightness temperatures will be changing over the satellite lifetime, the annual cycle of 2012 is simulated at each of the three locations. By simulating the annual cycle, the range and sensitivity of TIRS variations can be identified at each location. The seasonal changes in brightness temperatures are captured and analyzed, and the presence of inversions is also identified and analyzed. The following section presents the surface observational temperature timeseries, which gives a general idea of the variations we can expect in the TIRS at each location. Then, a comparison between the high-spectral PCRTM output and the PREFIRE-specific TIRS output is made. An analysis is then done of the annual variability found in the TIRS output and the impact on TIRS outputs when there is an inversion present. Finally, a timeseries of three important TIRS channels (the 11.4 μm transparent window channel, the 22.4 μm dirty window channel, and the 35.0 μm water vapor channel) is plotted and analyzed for each location.

3.1.1 Surface temperature

In order to get an idea of the variation in TIRS outputs for each of the locations, the 2012 surface temperature is plotted in Figure 3.1. From left to right, the surface temperatures are for Dismal Island, Summit Station, and Dome C II.

Dismal Island exhibits the warmest temperatures and least annual variations on average, with the maximum temperature occurring on February 6 at 10 Z of 5.6 °C. This makes sense considering this station is the lowest elevation of the three, and the most coastal station, so it is

influenced by maritime air more than inland stations like Summit Station and Dome C II. The average 2012 surface pressure for this station is 983 hPa. We can expect that the TIRS sensors in transparent window channels and dirty window channels will experience variations similar to the surface temperature variations. We can also expect this station to experience the least annual variability and the warmest temperatures.

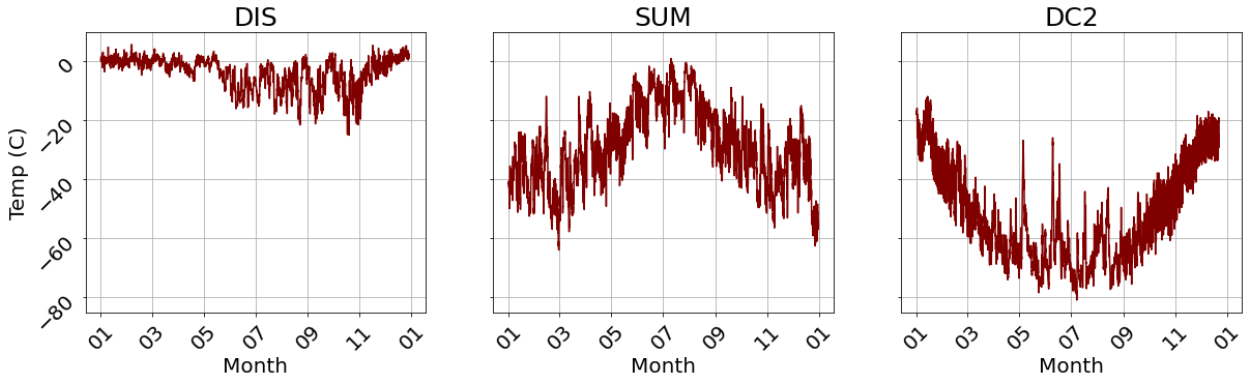

Figure 3.1: Surface temperature plotted for the year 2012 for Dismal Island (left), Summit Station (center), and Dome C II (right).

Summit Station, which sits at a higher elevation than Dismal Island and is an inland location, has a clear annual cycle of temperatures coldest during the winter and warmest in the summer. During the 2012 surface melt event that happened on Greenland's ice sheet, the warmest 2012 temperature was recorded at Summit Station of 0.82 °C on July 10 at 4 Z. The average 2012 surface pressure for this station is 662 hPa. This gives insight into what the general TIRS variability may look like at this location, with a clear seasonal cycle of brightness temperatures colder than Dismal Island but warmer (colder) than Dome C II in the northern hemisphere summer (winter).

Dome C II, the highest elevation station of the three locations and an inland site, also exhibits a clear annual cycle with the coldest temperatures in the austral winter and warmest in the austral summer. This station exhibits the coldest temperature recorded from the three stations for the year 2012 at -81.0 °C on July 7 at 15 Z. The average 2012 surface pressure for this station is

649 hPa. The TIRS measurements at this location can be expected to be colder than the other two locations, and will also experience a clear seasonality like Summit Station but unlike Dismal Island. Both Dome C II and Summit Station exhibit greater seasonality than Dismal Island, so a prediction can be made that these two inland stations will experience a higher range of TIRS brightness temperature outputs than Dismal Island.

3.1.2 High-spectral PCRTM vs TIRS output

For the year 2012, there was a total of 732 samples ran with PCRTM to simulate what the PREFIRE TIRS will observe at each location. The simulated output from the high-resolution PCRTM and the lower-resolution TIRS output were plotted against each other for each location and compared to gain insights into the range capabilities and accuracy of the simulated TIRS sensors. The comparison results are shown in Figure 3.2.

By examining the plot of the high-resolution PCRTM output versus the lower-resolution TIRS output, we can observe that despite the reduced spectral resolution, the TIRS sensors capture the range of variations observed in the PCRTM outputs. This finding shows that the PREFIRE mission is a capable and reliable mission for providing valuable information about the radiative characteristics of the observed scenes, despite its TIRS having a lower resolution.

The comparison between the PCRTM and TIRS outputs gives insight into the temperature trends of the three locations. Dismal Island experiences the warmest brightness temperatures while Dome C II exhibits the coldest temperatures. Summit Station falls within an intermediate range of temperatures when compared to the other stations. These temperature patterns highlight the distinct radiative characteristics of each location, demonstrating the capacity of the PREFIRE TIRS sensors to accurately capture and discern these unique characteristics.

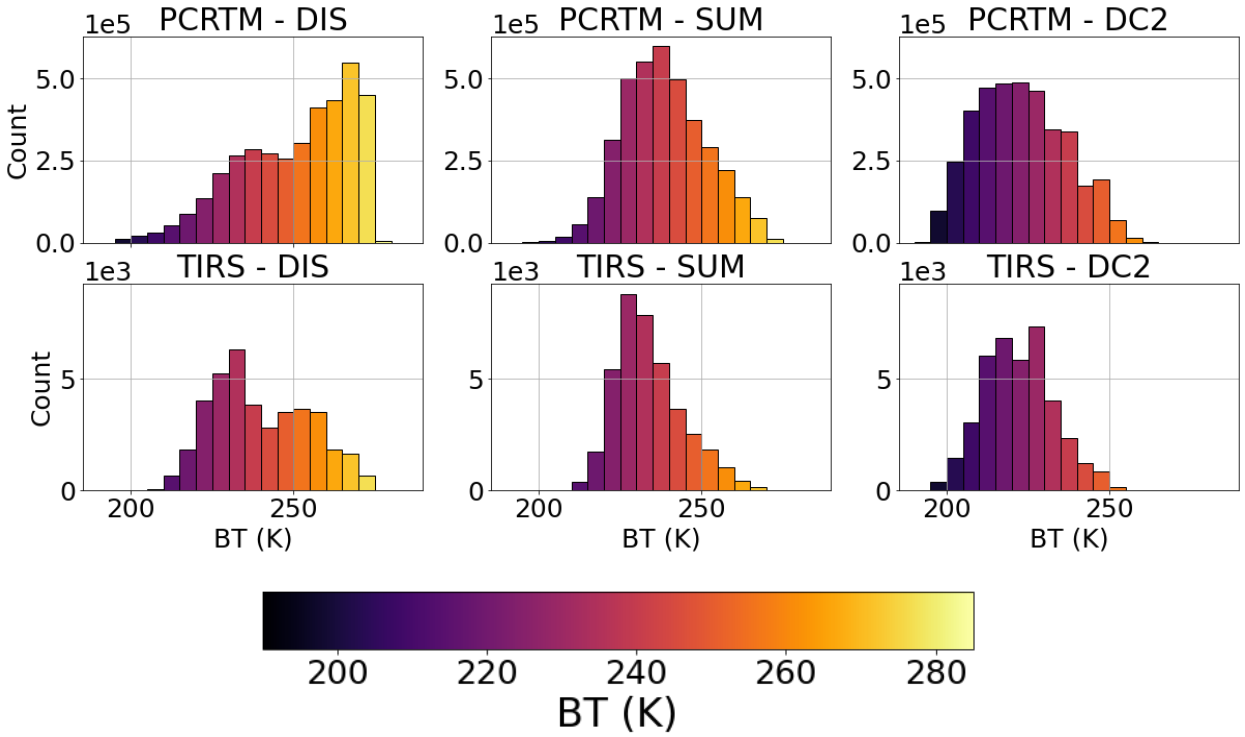

Figure 3.2: High-resolution PCRTM output (top row) compared to lower-resolution TIRS output (bottom row) for Dismal Island (left), Summit Station (center), and Dome C II (right).

3.1.3 TIRS annual variability

Each location has distinct ranges and characteristics of their annual TIRS simulated outputs. To see which station has the least and most variability during the simulated 2012 year, the 54 TIRS channel outputs of brightness temperatures were plotted and connected with a line and colored by their respective season, and the plots for each station can be seen in Figure 3.3 with Dismal Island being on top, Summit Station in the center, and Dome C II on the bottom.

The TIRS responses simulated at Dismal Island, the warmest and moistest location, exhibit the least variability when compared to the other two stations. The lines consistently follow a general pattern of the transparent window (11-12 μm) being warmer than the semi-transparent window (18-25 μm), which is generally warmer than the values in the water vapor channel (>25

μm). Since this station is very moist, the variability in brightness temperature retrievals is not very high, and the retrievals follow a consistent pattern with a comparatively low range of brightness temperatures. We can therefore expect the PREFIRE mission to measure a pattern similar to these TIRS responses over Dismal Island after launch.

Summit Station, which is more inland than Dismal Island and experiences colder temperatures and drier conditions, has a larger range in its simulated TIRS brightness temperature outputs. In the warmer months like the summer seasons, its pattern is like that of Dismal Island, where the warmest brightness temperatures occur in the transparent window channel and the coldest brightness temperatures occur in the water vapor channels. There are a few lines that have the opposite pattern, which can be seen in the bottom of the Summit Station plot in the blue winter months, where the transparent window channel and the semi-transparent window channel appear to have colder temperatures than the water vapor channel. This pattern also reveals itself more prominently in Dome C II's outputs, and it will later be analyzed and concluded to be the result of inversion presence. The range of brightness temperatures seen in Summit Station can be taken as a prediction as to what the PREFIRE TIRS instruments will measure annually over Summit Station.

Dome C II has a much higher spread in brightness temperatures than Dismal Island and exhibits the coldest temperature outputs, which makes sense considering this station experienced the coldest temperatures of the three stations for 2012 and it is a very dry location, making more of the outputs able to see further into the atmosphere than Dismal Island, which has water vapor impacting those retrievals. The pattern that was seen with Summit Station of the brightness temperatures being coldest in the transparent window channel and warmest in the water vapor channels is found to be the result of inversions, which will be discussed in the next section.

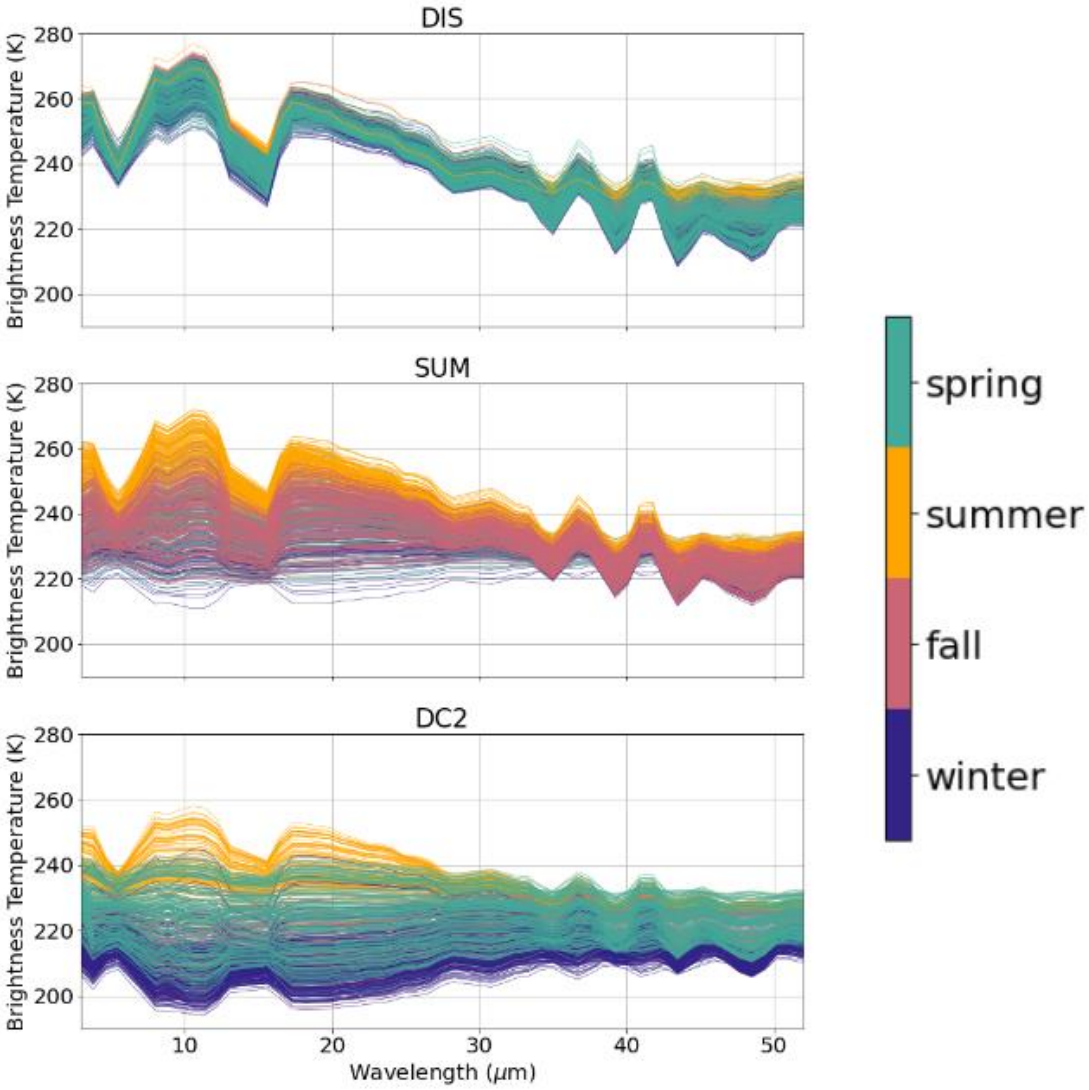

Figure 3.3. Brightness temperature output for the 54 PREFIRE-specific TIRS channels where each line is one output of the 732 samples for the year 2012 for Dismal Island (top), Summit Station (middle), and Dome C II (bottom), organized by season where green is spring, orange is summer, red is fall, and blue is winter.

The observed patterns in TIRS brightness temperatures across the three stations, with Dome C II exhibiting the highest spread and the coldest outputs, Dismal Island exhibiting the least spread and the warmest outputs, and Summit Station resting in between these two extremes, are consistent

with the climatic conditions of each location. These insights provide valuable predictions for what we can expect from the PREFIRE TIRS measurements post-launch.

3.1.4 Inversion presence

The presence of inversions, characterized by temperature increasing with height instead of decreasing, can significantly affect the retrieval of brightness temperatures by the PREFIRE TIRS. To understand the impact of inversions, Figure 3.4 illustrates an example TIRS output for the 54 channels compared to the temperature and water vapor profile inputs for Dismal Island, a location that did not experience an inversion in the sampled data from 2012. Additionally, a weighting function is plotted on the right side of the figure to identify regions of absorption in the atmosphere that the TIRS would be sensitive to.

Three representative TIRS channels were selected to analyze: the transparent window channel at 11.4 μm, the dirty window channel at 22.4 μm, and the water vapor channel at 35.0 μm. By matching these output TIRS brightness temperatures with the corresponding temperature profile inputs, the types of atmospheric conditions can be discerned by the TIRS outputs. Furthermore, the channels are plotted alongside the water vapor profile input with the three chosen channels aligned with the pressure levels of the temperature profile, allowing for the influence of water vapor on the TIRS retrievals to be examined.

In this first case of Dismal Island, which did not experience an inversion, the water vapor profile input plot confirms that this is the moistest station. Analyzing the weighting function reveals the regions in the atmosphere where each channel exhibits its sensitivity and where their retrieval is most influenced by absorption or lack thereof. Areas of increasing weighting function correspond to absorption taking place. The 11.4-μm TIRS channel displays negligible absorption

throughout the atmosphere except for some minimal absorption near the surface, indicating its low sensitivity to water vapor in the lower atmosphere. In contrast, the 22.4-µm TIRS channel exhibits a significantly higher increase in the weighting function around the 600-hPa level, consistent with the temperature input sounding. Similarly, the 35.0-µm TIRS channel shows its peak in the weighting function just above 400-hPa, in agreement with the temperature input sounding. These weighting functions highlight that the water vapor channel and semi-transparent window channels associated with PREFIRE TIRS are particularly responsive to even small amounts of water vapor in the atmosphere.

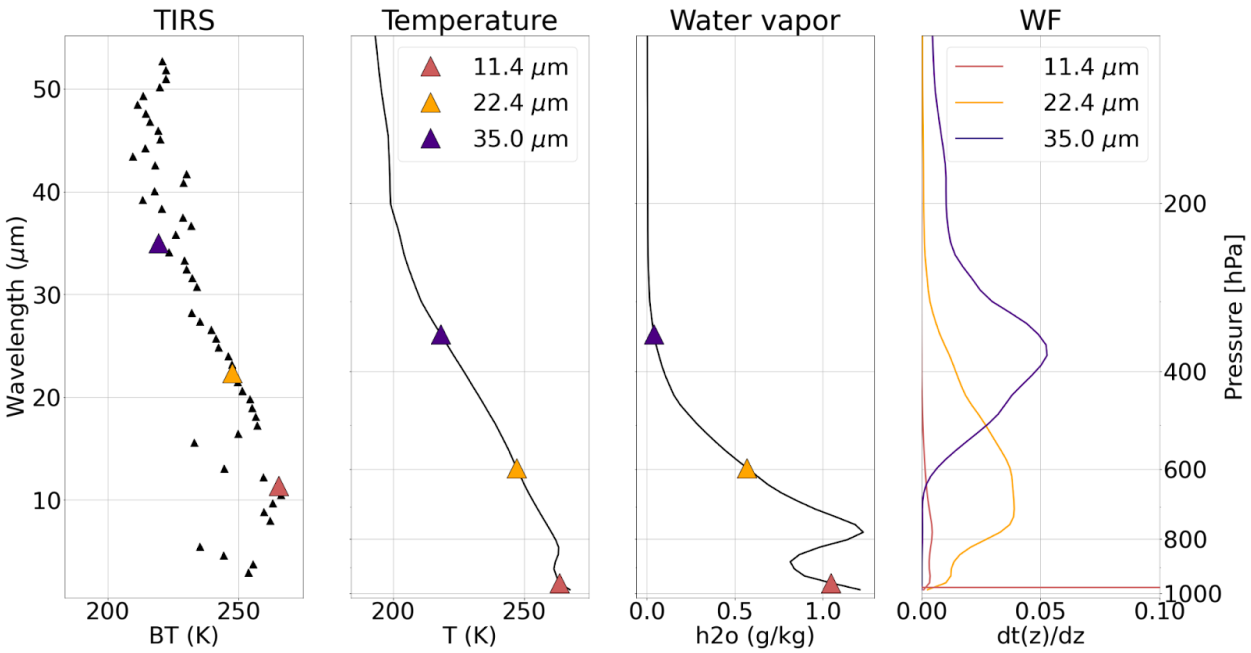

Figure 3.4. The 54 TIRS channel brightness temperature outputs versus wavelength (left), the temperature profile input versus pressure (second from left), the water vapor profile input versus pressure (second from right), and the associated weighting function versus pressure (right) for Dismal Island on July 5, 2012, at 0 Z. The three chosen channels to analyze are the 11.4-micron transparent window (purple), the 22.4-micron dirty window (orange), and the 35.0-micron water vapor channel (red).

Figure 3.5 shows an example similar to that shown in Figure 3.4, but for Dome C II, which is a dry inland station that experienced an inversion during the same day and time.

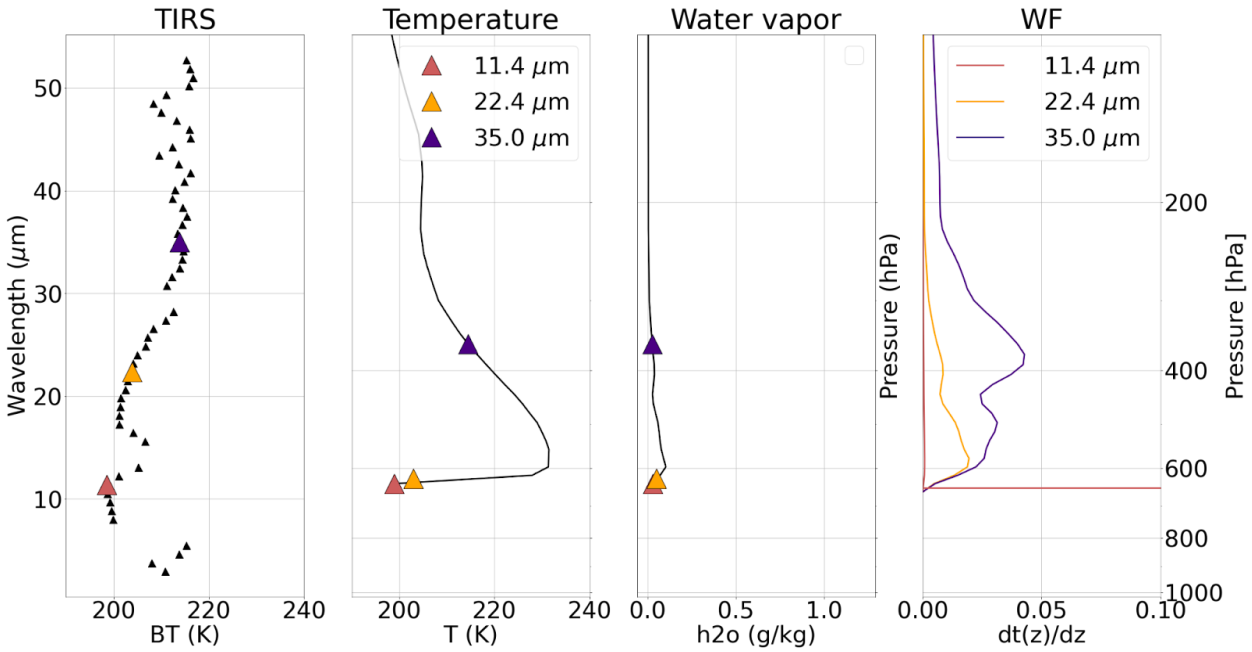

Figure 3.5. The same as in Figure 3.4, but for Dome C II.

In this case, Dome C II exhibits a pronounced temperature inversion near the surface, as evident from the temperature profile input. Notably, the TIRS output brightness temperature of the transparent window channel corresponds to the surface temperature, which now registers as the coldest temperature of the three chosen TIRS channels due to the inversion.

When examining the weighting function, negligible absorption above the surface is observed in the 11.4-µm transparent window TIRS channel. Comparatively, the 22.4-µm dirty window TIRS channel exhibits less absorption by water vapor when compared to the example at Dismal Island. For Dome C II, the dirty window TIRS channel reaches its peak just above the surface, indicating that the TIRS output at the 22.4-µm TIRS channel occurs slightly above the surface, appearing warmer than the surface itself due to the presence of the inversion. In contrast, the 35.0-µm water vapor TIRS channel maintains its peak around 400 hPa, similar to the Dismal Island case, as this TIRS channel is particularly responsive to even minor amounts of water vapor

in the atmosphere. Consequently, the TIRS output at the 35.0-μm channel displays the highest temperature when compared to the 11.4 and 22.4-μm channels, reflecting the influence of the inversion.

Each of these three chosen TIRS channels gives valuable information about different levels of the atmosphere. Next, the three TIRS channels are compared to each other for each location on an annual timescale. A comparative analysis of these TIRS channels, along with the surface temperature timeseries, unveils the 2012 annual variations in PREFIRE measurements within the chosen channels.

3.1.5 Timeseries of 3 TIRS channels

In order to examine the temporal variations of the three selected TIRS channels (11.4-μm transparent window, 22.4-μm dirty window, and 35.0-μm water vapor channel) along with surface temperature throughout the year 2012, a timeseries analysis is performed. The timeseries plots were generated for each station and can be seen in Figure 3.6 with Dismal Island on top, Summit Station in the middle, and Dome C II on the bottom.

The analysis reveals distinct patterns in the behavior of the three TIRS channels across the three stations. Firstly, the 11.4-μm transparent window TIRS channel exhibits a consistent correlation with surface temperature values at all stations, demonstrating a close relationship between the two. This makes sense considering this TIRS channel is always measuring near-surface temperatures in the absence of clouds, which are not included in the simulations of this section.

Conversely, the 22.4-μm dirty window TIRS channel closely tracks surface temperature at the drier stations, Summit Station and Dome C II, while its association weakens for Dismal Island

due to the high moisture content on the peninsula. At Dismal Island, this TIRS channel exhibits a greater sensitivity to the middle atmosphere rather than the surface, reflecting the influence of abundant water vapor on retrievals.

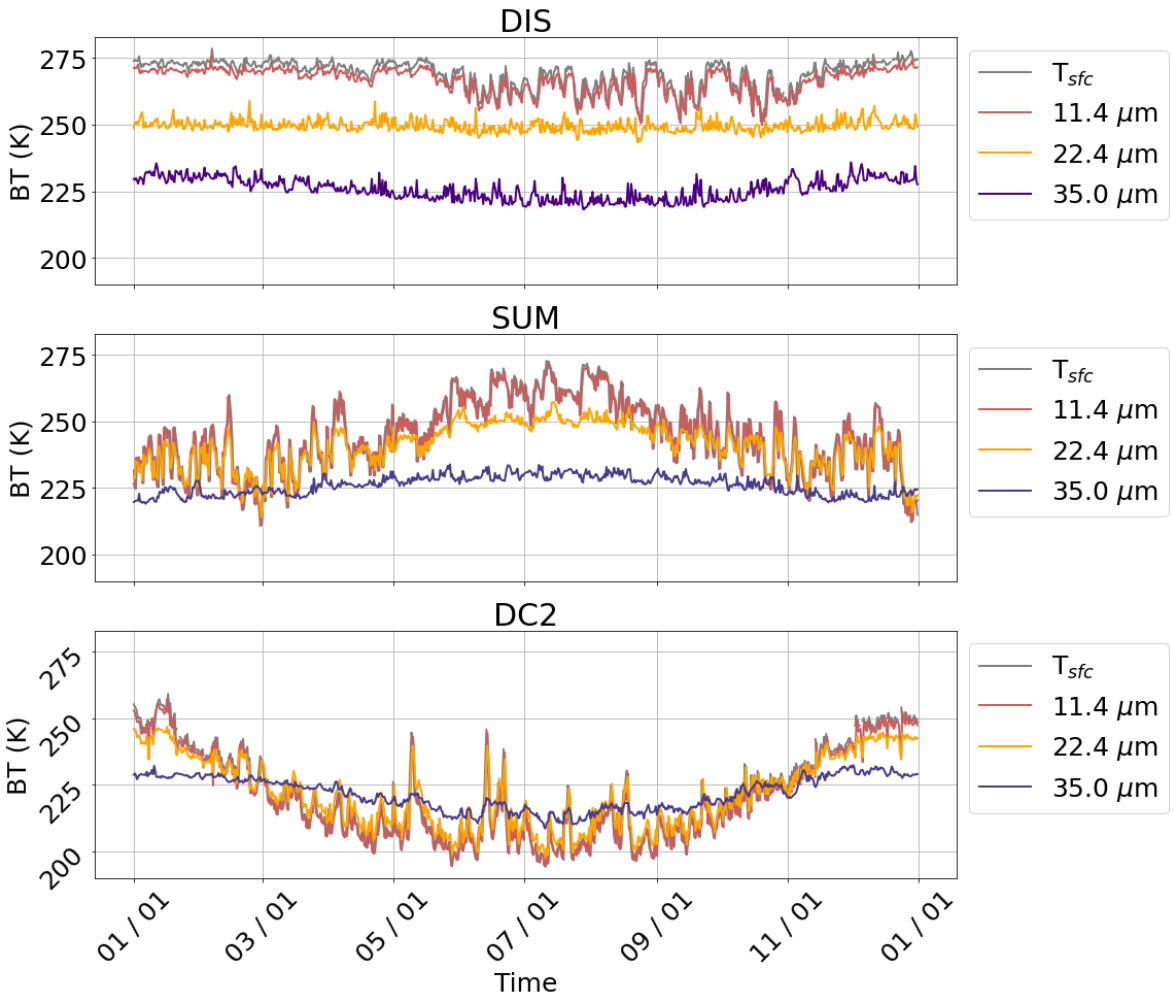

Figure 3.6. Timeseries of the surface temperature (gray), the TIRS output 11.4-μm transparent window channel (red), 22.4-μm dirty window channel (orange), and 35.0-μm water vapor channel (purple) for Dismal Island (top), Summit Station (middle), and Dome C II (bottom) for the year of 2012.

In contrast, the 35.0-μm water vapor TIRS channel displays minimal variation with the surface temperature across all stations. While it exhibits slight seasonal variability, this TIRS

channel is primarily capturing the sensitivity of small amounts of water vapor in the high atmosphere, rendering it insensitive to surface variations. Notably, during inversions, the water vapor channel can be warmer than the other two channels, as observed in the plots for Summit Station and Dome C II but not in the case of Dismal Island.

This section has presented the annual TIRS variations simulated at each of the three locations for the year 2012, revealing distinct TIRS brightness temperature signatures in the chosen channels. The comparison between each station reveals the role of water vapor on TIRS retrievals, where the dirty window and water vapor TIRS channels will be more sensitive to the presence of water vapor. Inversions and their influence on the TIRS retrievals have also been identified and discussed, where the transparent window channel may read a colder brightness temperature than both the dirty window and water vapor channel retrievals. These simulations serve a crucial purpose in the context of the PREFIRE satellite mission, as they allow us to anticipate and understand the expected variability and behavior of the TIRS sensors at different polar locations.

3.2 Surface emissivity

In polar climates, the accurate characterization of surface emissivity plays a crucial role in understanding the radiative properties of different surface types. In this section, an analysis is done to determine the PREFIRE TIRS sensitivity during three distinct events: a surface freeze event at Dismal Island, the Greenland surface melt event, and a katabatic wind event at Dome C II. By analyzing the radiative impact of these changing surface types, their influence on TIRS retrievals can be determined. Understanding the variations in surface emissivity in polar regions enables us to accurately interpret the far-infrared thermal signals and enhance our ability to monitor polar environments using remote sensing. The effect of changing surface types is analyzed in this section

to understand the impact of their radiative properties on TIRS retrievals, which can help us predict the PREFIRE sensitivity to changing surface types. This section will also refer to surface emissivity differences in the far-infrared, and a plot of these values can be found in figure 2.5.

3.2.1 Surface freeze event

The first event examined focuses on the differences between a water surface and an ice surface at the Antarctica Peninsula location of Dismal Island. By investigating the radiative properties of these two surface types, the potential behavior of the PREFIRE TIRS measurements during a surface freeze event can be better understood and anticipated. Figure 3.7 shows the plot of the difference between TIRS outputs when the surface is water versus ice. The brightness temperature differences that will be focused on are three distinct areas of the far-infrared spectrum – the transparent window, the dirty window, and the water vapor TIRS channels.

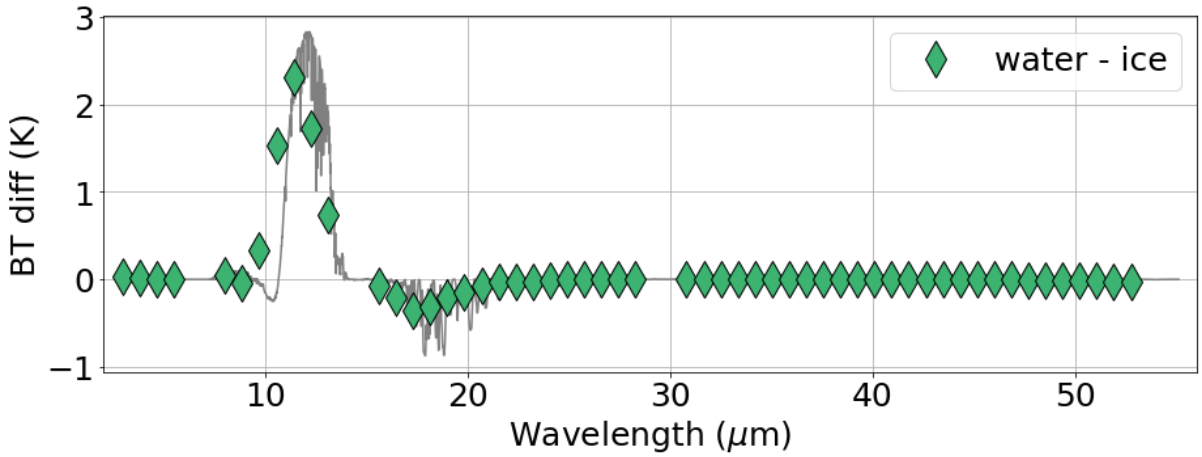

Figure 3.7. The difference in TIRS brightness temperature outputs (green diamonds) with the high-spectral PCRTM output (gray line) for Dismal Island between a water surface output and an ice surface output.

The most significant sensitivities are observed in the transparent window channel, between 11-12 μm. At 11.4 μm, the TIRS brightness temperature difference is 2.3 K, corresponding to an emissivity difference of 0.04. This indicates that a water surface would cause more radiation to reach the PREFIRE sensors in the transparent windows than if there was an ice surface present.

There is slight sensitivity in the dirty window channel, where the TIRS brightness temperature difference at 22.4 μm is -0.02 K, associated with an emissivity difference of -0.03. Although this indicates that an ice surface would cause more radiation to reach the satellite, this difference is negligible as it is on the order of 0.01 K. A difference this small would be difficult to detect by even a very high-resolution satellite.

Beyond 20 μm, the sensitivity diminishes considerably and is also negligible to the PREFIRE TIRS and other higher-resolution satellites. The brightness temperature difference at 35.0-μm is -0.0004 K associated with an emissivity difference of -0.05. These findings indicate that higher emissivity differences do not necessarily result in larger brightness temperature differences. Given Dismal Island's high moisture content, the presence of water vapor affects brightness temperature retrievals across the entire spectrum and renders wavelengths longer than 20 μm insensitive to surface emissivity changes. While the PREFIRE TIRS will be able to capture surface emissivity differences in the transparent window channels at Dismal Island during a surface freeze event, differences below 1 K at longer wavelengths may not be discernible by the PREFIRE mission with just one measurement.

3.2.2 Greenland surface melt event

The next event analyzed is the Greenland surface melt event at Summit Station, where the difference is taken between the PREFIRE TIRS outputs for a fine snow surface and a water surface,

plotted in Figure 3.8. The brightness temperature differences are explored for the same three transparent/absorption TIRS channels that were identified at the beginning of the previous section.

Similar magnitudes of brightness temperature sensitivities are found in the transparent and dirty window channels less than 20 μm. In the transparent window channel, the difference is 0.6 K at 11.4 μm, associated with an emissivity difference of 0.03. Although this difference is less than the threshold of what the PREFIRE TIRS can capture in a single measurement, an event like this could be identified with many measurements, as the error decreases with increasing measurements. This positive difference indicates that a fine snow surface would result in higher radiation reaching the satellite sensors than a water surface.

At 22.4 μm, in the dirty window channel, the difference is 0.04 K which corresponds to an emissivity difference of 0.07. Like in the transparent window, this would indicate that a fine snow surface would cause more radiation to reach a satellite sensor in this portion of the spectrum, but this difference is not within the range of what PREFIRE nor a higher-resolution satellite could measure based on a single scene, so this difference is negligible.

Beyond 20 μm, the sensitivity differences are also negligible, despite fine snow and water emissivity having the largest differences in the water vapor portion of the spectrum. The output TIRS difference at 35.0 μm is 0.01 K, associated with an emissivity difference of 0.09. The water vapor influences the retrievals in this area of the spectrum due to its strong absorption, so surface radiation is not reaching the satellite sensors beyond 20 μm. Though these differences provide valuable insight into the effects of a fine snow surface versus a water surface at Summit Station, all the differences remain below the 1 K threshold that PREFIRE can detect with a single measurement. With more measurements and statistics, this error will decrease, so a higher sample

size could result in the PREFIRE TIRS able to detect these surface emissivity differences, especially in the transparent window where the highest sensitivities occur.

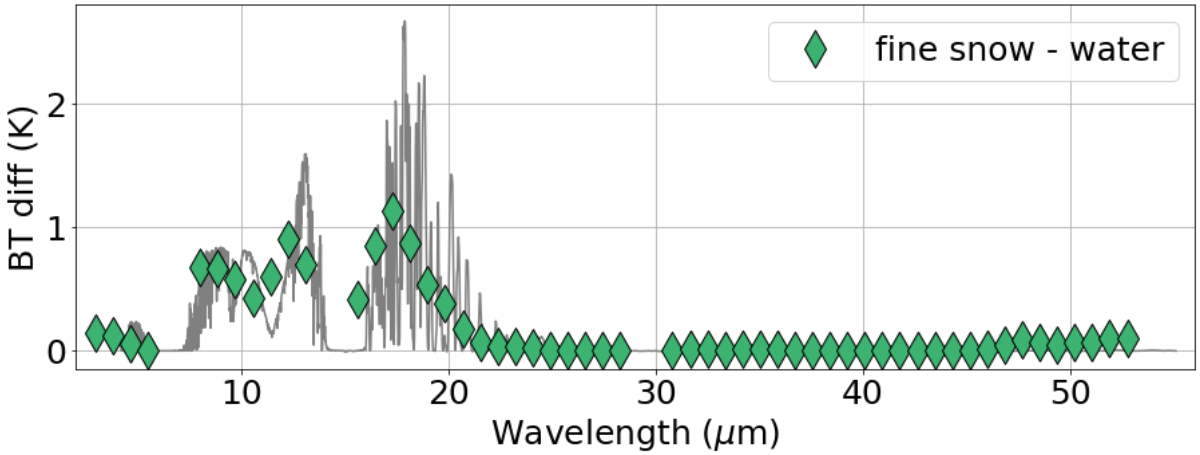

Figure 3.8. The difference in TIRS brightness temperature outputs (green diamonds) with the high-spectral PCRTM output (gray line) for Summit Station between a fine snow surface output and a water surface output.

3.2.3 Katabatic wind event

The last simulation done in this section explores the effect of high katabatic winds changing the surface type at Dome C II from medium snow to fine snow. During this event, winds reached nearly 10 m s^{-1} at Dome C II, which changes snow emissivity by causing the snowflakes to become less dendritic, more spherical, and finer. The goal of this section is to determine where in the far-infrared spectrum the PREFIRE TIRS will be sensitive to surface snow type changes, and to what magnitude the TIRS will be sensitive. The results are plotted in Figure 3.9, and the following analysis will focus on the three important transparent/absorption channels identified at the beginning of section 3.2.1.

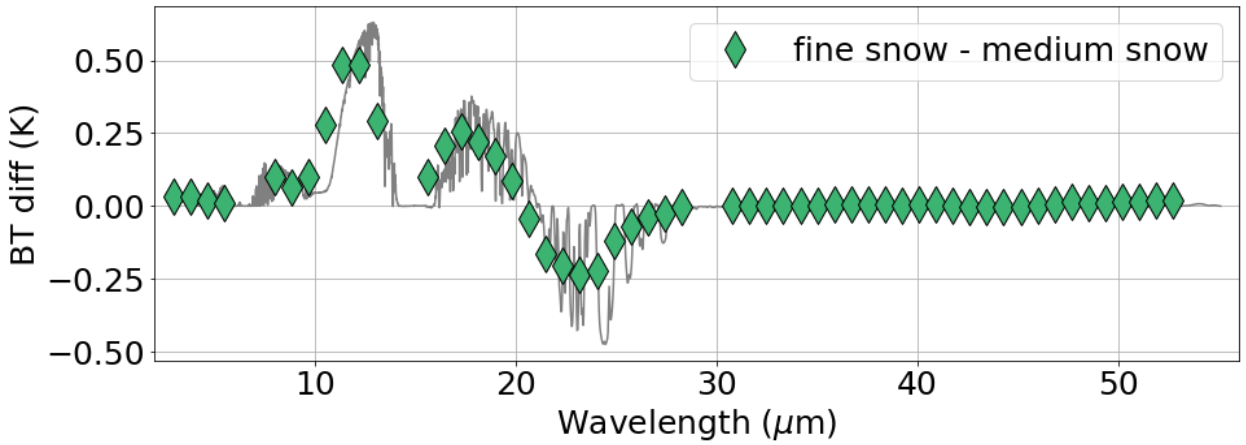

Figure 3.9. The difference in TIRS brightness temperature outputs (green diamonds) with the high-spectral PCRTM output (gray line) for Dome C II between a medium snow surface output and a fine snow surface output.

The largest sensitivities in this TIRS simulation appear in the transparent and dirty window channels less than 30 μm. At 11.4 μm, the brightness temperature difference is 0.5 K, associated with an emissivity difference of 0.07. This indicates that a fine snow surface would cause more radiation to reach the satellite sensors than a medium snow surface in the exact same atmospheric conditions at Dome C II. This difference may not be detectable with just one PREFIRE TIRS measurement, but with many measurements, a fine snow surface could be discerned from a medium snow surface in the transparent window TIRS channel.

In the dirty window channels, specifically at the 17.3 μm and the 23.2 μm TIRS channels, the differences in brightness temperature outputs are 0.26 K and -0.24 K, respectively. This indicates that more radiation from the surface would reach the satellite at 17.3 μm from a fine snow surface, but more radiation from a medium snow surface would reach the satellite in the 23.2 μm TIRS channel due to the emissivity differences also switching from positive to negative. This sensitivity may be negligible to PREFIRE, but higher-resolution satellites may be able to resolve the difference between these two surfaces on the polar plateau.

The differences become negligible beyond 30 μm. At 35.0 μm, the difference is 0.0003 K with an emissivity difference of 0.0009. This is a very small sensitivity that the PREFIRE TIRS would not be able to detect, nor even the highest-resolution satellite.

Since Dome C II is a very dry location, there is more sensitivity at higher wavelengths that the simulated PREFIRE TIRS measurements can resolve. In the previous surface simulations, the sensitivity was only present at wavelengths less than 20 μm. Though, similarly to the Greenland melt event simulation, these differences of a simulated katabatic wind event are less than 1 K, so a surface change from medium snow to fine snow is not something that PREFIRE is expected to be able to resolve with just one measurement. Again, PREFIRE may be able to resolve these types of events with many measurements as the brightness temperature threshold error decreases with increasing samples.

These simulations reveal that the sensitivity of TIRS to surface type changes depends on the surface emissivity differences as well as the transparency of the atmosphere, with water vapor channels being the least sensitive to the change and transparent and dirty window channels most sensitive to the change. A surface change between a water surface and ice surface at Dismal Island caused the highest TIRS sensitivity in the transparent window channels with low TIRS sensitivity at higher wavelengths. When simulating the Greenland surface melt event with a fine snow surface difference between a water surface, there are differences in the PREFIRE measurement threshold of 1 K in the transparent window and dirty windows, but again, the sensitivity drops off to be negligible at longer wavelengths. For a katabatic wind event where the surface changes between more dendritic, larger snow particles to less dendritic, finer snow particles, the highest TIRS sensitivity occurs in the transparent window and some TIRS sensitivity in the dirty window channels until about 25 μm, where the sensitivity becomes negligible due to high water vapor

absorption at longer wavelength channels. Even where the TIRS are sensitive to a simulated katabatic wind event at Dome C II, the sensitivities are less than what the PREFIRE TIRS can resolve in one scene.

3.3 Cloud sensitivity

All polar clouds are important for our understanding of polar energy imbalances. Many different types of clouds exist in polar climates, and characterizing them in terms of how the PREFIRE TIRS will measure them is important to get an insight into their radiative properties. The far-infrared is sensitive to not only cloud presence but also cloud phase. While liquid clouds and mixed-phase clouds are prevalent along the coasts of Antarctica and throughout the entirety of Greenland, the far-infrared spectrum is especially sensitive to optically thin ice clouds, especially in the dry environments of polar regions. By examining how the TIRS will measure all cloud types, their radiative behavior and contribution to the overall global energy balance can be better understood.

In this section, TIRS responses to general cloud presence are analyzed by comparing spectra of ice clouds versus clear sky at Dome C II, ice clouds versus mixed-phase clouds at Summit Station, and ice clouds versus liquid clouds at Dismal Island to determine how the far-infrared spectrum reacts to cloud presence and cloud phase. All these general cloud presence simulations are done in the mid-level atmosphere at 5 km above the surface. Then, additional cloud simulations are performed for low-level, mid-level, and high-level clouds with varying effective radii and ODs. Each section will include a cloud simulation at the three locations: Dismal Island, Summit Station, and Dome C II, and will specify whether the cloud simulated is liquid, mixed-phase, or ice. Special cases that exist at Dome C II – low-level diamond dust and high-level polar

stratospheric clouds – are also simulated. Each simulation will compare the same cloud at the same location with changing effective radius, then with changing OD. Dismal Island will include simulations that compare the same types of clouds in summer versus winter. All these simulations are important to fully characterize how cloud signatures will appear to the PREFIRE TIRS measurements.

3.3.1 Cloud presence and cloud phase

In order to understand how clouds will affect the far-infrared spectrum in comparison with a clear sky, the first simulation focuses on mid-level ice clouds over Dome C II. The ice clouds are set at 5 km above the surface with an OD of 1 and an effective radius of 15 μm, and then their resulting TIRS signatures are subtracted from that of clear sky conditions at the same date and time. The result is shown in Figure 3.10.

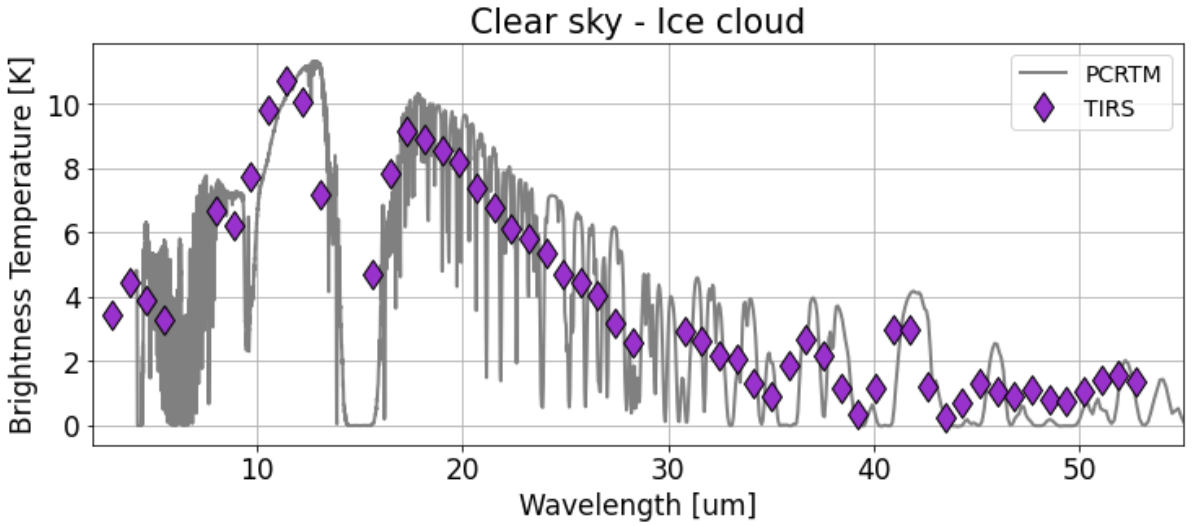

Figure 3.10. The difference in TIRS (diamond markers) between a clear sky and a mid-level ice cloud over Dome C II during the austral summer. The high-resolution PCRTM output (gray line) is included.

In this dry, high-plateau environment, almost all the TIRS channels have a sensitivity to thin ice clouds. The fact that all the differences are positive indicates that the presence of an ice cloud would result in less radiation reaching the satellite than that of a clear sky environment. The shorter wavelength TIRS channels less than 10 μm have sensitivities above 3.0 K to a thin ice cloud present. The highest sensitivities occur in the transparent window channel around 11.4 μm, where the difference exceeds 10 K, meaning that even a thin ice cloud will obscure the surface signal in the PREFIRE measurements. Similarly in the dirty window channels between 15 μm and 30 μm, there are large differences that start at 9.0 K and decrease to 3.0 K. These differences would be noticeable to PREFIRE, meaning the TIRS will be sensitive to even very thin ice clouds. There are even differences in the longer wavelength water vapor TIRS channels beyond 30 μm that range from 0 K to 3 K, and PREFIRE may be sensitive to differences above 1 K. This result indicates that extremely dry areas like Dome C II will be very sensitive to cloud presence, even clouds with small ODs.

The next two simulations are to determine the sensitivity of the PREFIRE TIRS to different cloud phases of the exact same ODs and effective radii. The first cloud simulation compares ice clouds and mixed-phase clouds at Summit Station. Both clouds have the same effective radius of 15 μm and OD of 10, and the difference between the resulting spectra is shown in Figure 3.11.

There are no longer significant TIRS differences in the transparent window like we saw in the previous simulation, but instead, the dirty window channels and water vapor channels are sensitive to these two different cloud phases. The largest difference of 3.5 K occurs in the 22.4 μm dirty window TIRS channel. These positive differences in the dirty window channels indicate that a mixed-phase cloud of the exact same physical properties as an ice cloud will result in more radiation reaching the satellite sensors. The differences in TIRS become negative and on the order

of -1.0 K when looking at the water vapor channels between 30 and 40 μm. The largest difference in this range reaches just above 1.0 K, indicating that PREFIRE would be able to resolve such a difference. The negative values indicate that an ice cloud would result in more radiation reaching the satellite than a mixed-phase cloud in the water vapor channels. These signatures in the dirty window and shorter water vapor channels provide a particularly clear example of the unique information the far-infrared spectrum provides for distinguishing between cloud phases. Beyond 43 μm, the TIRS differences are less than 0.5 K, meaning PREFIRE would not be able to resolve such signatures.

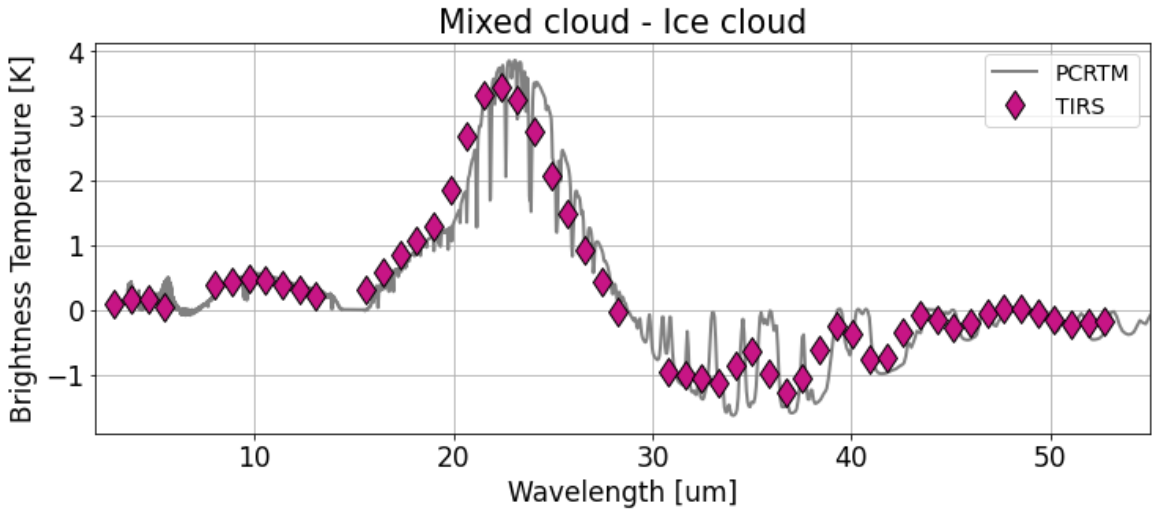

Figure 3.11. The difference in TIRS (diamond markers) between mid-level mixed-phase and ice clouds over Summit Station during the northern hemisphere winter. The high-resolution PCRTM output (gray line) is included.

The final simulation compares mid-level ice clouds and liquid clouds over Dismal Island. The clouds simulated have effective radii of 15 μm and an OD of 10. The result is shown in Figure 3.12.

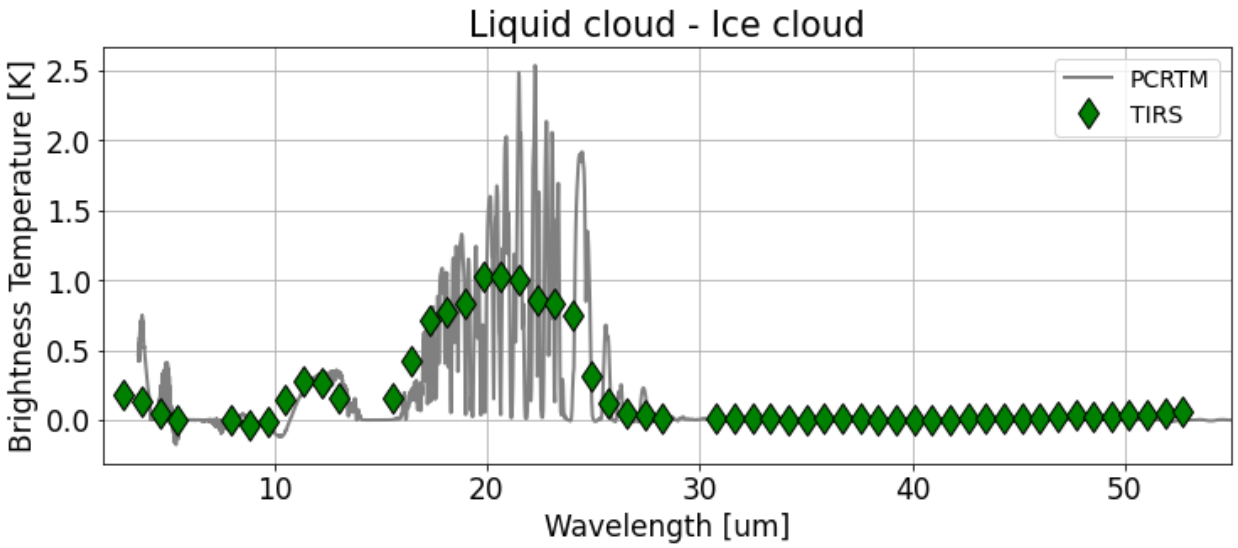

Figure 3.12. The difference in TIRS (diamond markers) between mid-level liquid and ice clouds over Dismal Island during the austral summer. The high-resolution PCRTM output (gray line) is included.

Significant TIRS differences (above 0.5 K) occur in the dirty window channel between the TIRS channels of 18.1 and 24.0 μm. These differences are positive, indicating that a liquid cloud of the same physical properties as an ice cloud would yield more radiation reaching the satellite sensors over Dismal Island. Unlike Summit Station, increased moisture at Dismal Island masks differences beyond 24.0 μm into the water vapor channels. These differences in TIRS are less than 0.5 K and are thus negligible to PREFIRE.

In the next sections, clouds are simulated at different levels in the atmosphere, and then they are compared to other clouds that are of the same physical properties except for changing effective radius or changing OD.

3.3.2 Low-level clouds

The first simulation examines low-level liquid clouds at Dismal Island, set at 1 km above the surface using the hypsometric equation (1) and the virtual temperature equation (2). Then,

every physical property of the cloud and the environment is kept constant except for the effective radius, which is changed between 5, 15, and 25 μm. The OD is kept constant at 10. The difference between each radius is taken at each simulated TIRS measurement, and then the same simulation is done 6 months later to determine how the cloud signatures vary by season. The result is shown in Figure 3.13.

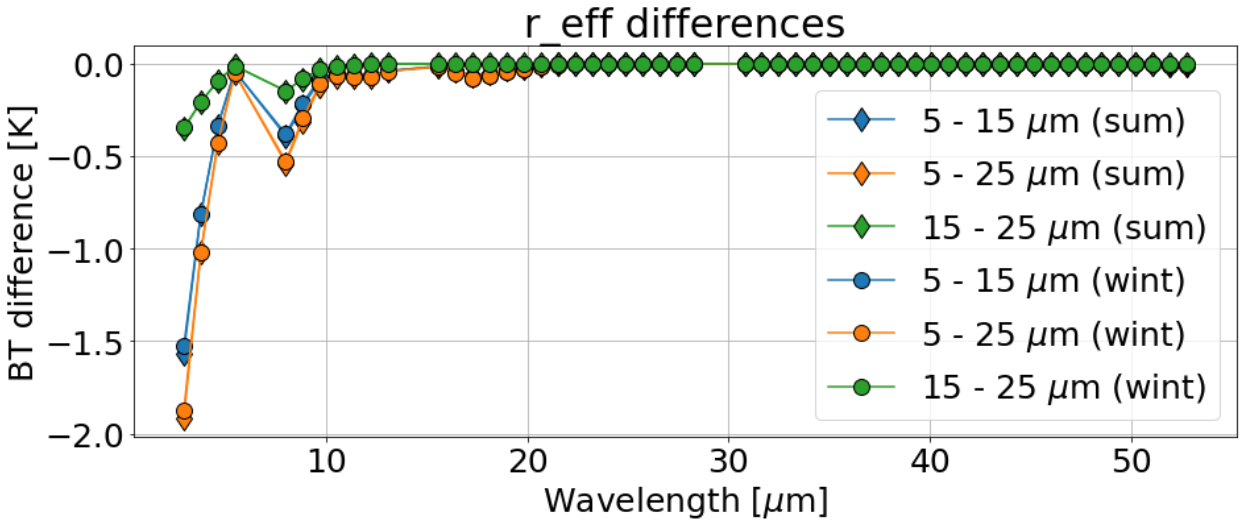

Figure 3.13. The differences in TIRS between 5, 15, and 25 μm at Dismal Island for a low-level liquid cloud during the austral summer (diamond markers) and winter (circle markers).

For both summer and winter, low-level liquid clouds over Dismal Island show sensitivity only in the shortest wavelength TIRS channels, with a maximum sensitivity of nearly -2.0 K occurring between the smallest and largest simulated effective radii of 5 and 25 μm at the 3 μm TIRS channel. There is also some sensitivity near the 9.6 μm ozone absorption channel. The sensitivity quickly drops off for all effective radii beyond 10 μm. Smaller effective radii yield colder brightness temperatures at these short wavelengths, reflecting the fact that cloud emissivity decreases with larger effective radii. These differences may be distinguishable by PREFIRE with one measurement since it is greater than the error threshold of 1 K. When comparing the summer versus winter differences in effective radii, the cloud signatures are largely insensitive to changes

in the environmental conditions between the seasons. Differences in effective radii in summer versus winter for low-level liquid clouds at Dismal Island will yield the same sensitivities in the same TIRS channels.

Next, the low-level liquid clouds are kept at a constant effective radius of 15 μm, but the OD is increased from 10 to 30. Again, this simulation is done for both summer and winter for Dismal Island. The result is presented in Figure 3.14.

Similarly to the effective radius result, this result shows that the signatures for changing between cloud ODs in the summer and winter yield the same TIRS signatures, but there is not a high sensitivity to increasing the OD beyond 10. Throughout the spectrum, the signatures are below the threshold that PREFIRE would be able to resolve, which shows that the infrared brightness temperatures are already saturated and insensitive to increasing OD. So, changing ODs between 10 and 30 at Dismal Island is not expected to yield a significant difference in TIRS signatures in any season.

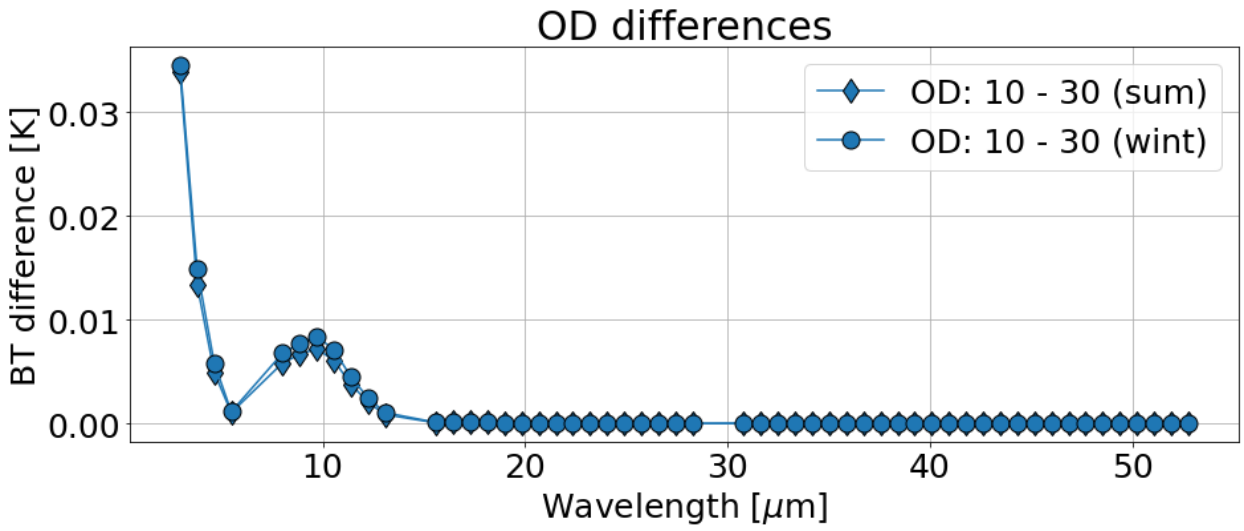

Figure 3.14. The differences in TIRS between ODs of 10 and 30 for a low-level liquid cloud during the austral summer (diamond markers) and winter (circle markers).

The next simulation done for low-level mixed-phase clouds is at Summit Station. The clouds are set at 1 km above the surface using the hypsometric equation, and then the effective radius is changed between 5, 15, and 25 μm with all other cloud properties remaining the same with a constant OD of 10. The result is presented in Figure 3.15.

Low-level, mixed-phase clouds at Summit Station of differing effective radii will yield TIRS sensitivities at shorter wavelengths below 10 μm, and then the highest sensitivities occur in the dirty window channels, especially near 20 μm. The sensitivities then drop off and become negligible beyond 30 μm, most likely due to water vapor absorption influencing the amount of radiation from a low-level cloud that could reach a satellite sensor. This result also shows that smaller effective radii will result in less radiation reaching the satellite, and higher effective radii will result in more radiation reaching the satellite across the whole spectrum. The highest difference occurs between 5 and 25 μm near the 20 μm TIRS channel. Summit Station exhibits more sensitivities across the far-infrared spectrum than we saw at Dismal Island due to the fact that the clouds contain ice in addition to liquid, and the above-cloud atmosphere is much drier at Summit Station, so there is less water vapor to influence TIRS retrievals of the clouds. These differences in effective radii reach and exceed PREFIRE's error threshold of 1 K, so it is likely that PREFIRE will be able to resolve differences in effective radii at shorter wavelengths and in the dirty window channel for low-level mixed-phase clouds at Summit Station.

To further determine TIRS sensitivity to cloud thickness at Summit Station, two additional simulations were conducted keeping the effective radius constant at 15 μm and changing the OD between 1 and 15. The result is plotted in Figure 3.16.

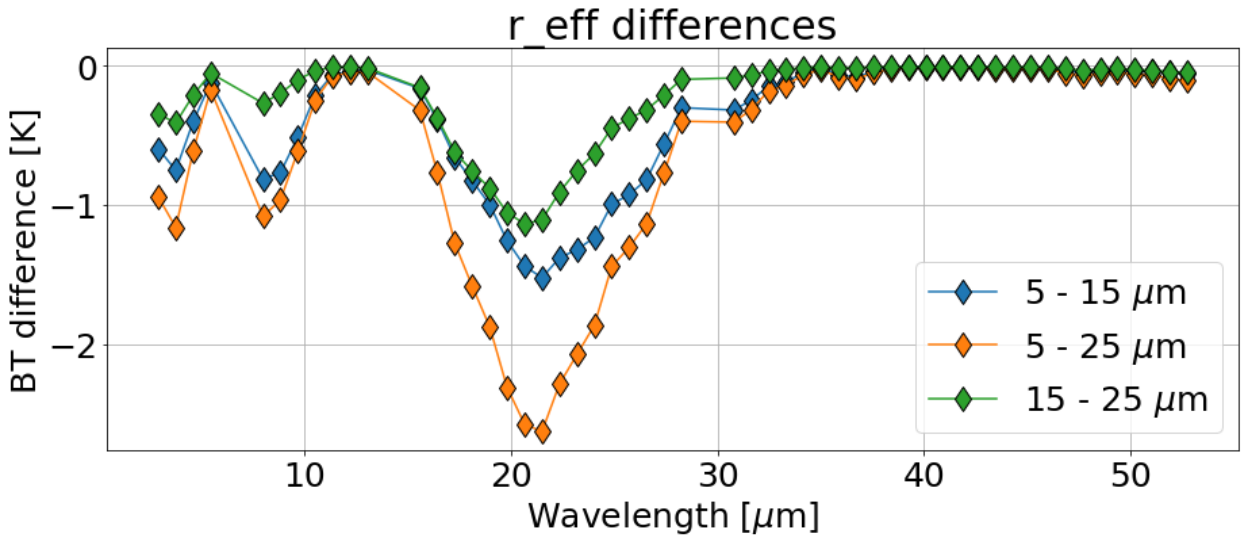

Figure 3.15. The differences in TIRS between 5, 15, and 25 μm at Summit Station for a low-level mixed-phase cloud during the northern hemisphere winter.

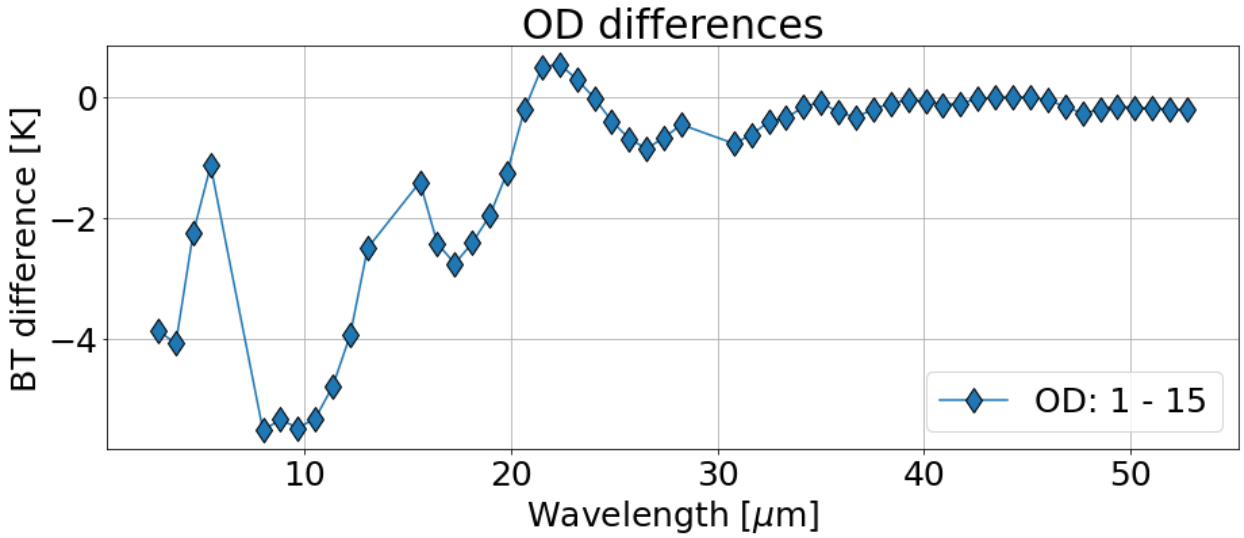

Figure 3.16. The differences in TIRS between ODs of 1 and 35 for a low-level mixed-phase cloud during the northern hemisphere winter at Summit Station.

There are TIRS sensitivities across the spectrum with many areas exceeding the PREFIRE error threshold. At shorter wavelengths is where the largest TIRS sensitivities are found between these ODs, especially near the 10 μm TIRS channels where the difference exceeds -5.0 K. In the transparent window channels, the sensitivities decrease but are still well above a 1.0 K magnitude.

In all TIRS channels below 20 μm, the differences are negative, indicating that a low-level mixed-phase cloud of OD of 1 will yield less radiation reaching the satellite than an OD of 15. This is the opposite of what was found previously in these areas of the spectra, where more radiation from a low-level cloud was reaching the satellite at other locations. This is due to the inversion present at this location, where the top of the cloud is sitting in an area of warmer temperatures than the surface. The thicker cloud is emitting more radiation that reaches the satellite than a thinner cloud due to the presence of this inversion, which can be seen in the sounding of Figure 3.17. There are positive differences in a few TIRS channels just above 20 μm that nearly reach 1 K, indicating that PREFIRE may not be able to resolve this OD difference with one measurement but could possibly resolve it with more measurements. Beyond 30 μm, the TIRS sensitivities decrease to less than 1 K, likely due to water vapor above the low-level cloud influencing the cloud radiation able to reach the satellite sensors.

Diamond dust is simulated for low-level clouds at Dome C II. Diamond dust is a very optically thin ice cloud that forms close to the surface, so these clouds are set at 0.25 km above the surface. The first simulation done for diamond dust changes the effective radius between 2, 12, and 1000 μm, where 12 μm is the average size of diamond dust particles. The OD is constant at 1 in these simulations. The result is shown in Figure 3.18.

The far-infrared spectrum in the dirty window channels may be sensitive to distinguishing larger diamond dust particles from smaller ice cloud particles at Dome C II. However, across the spectrum, the differences between effective radii for low-level diamond dust at Dome C II do not yield large enough differences to exceed the TIRS radiometric accuracy. The largest sensitivity occurs in the dirty window channel with a peak near 20 μm between effective radii of 2 and 1000 μm. Although these differences do no exceed 0.5 K, the far-infrared is still showing some

sensitivity to diamond dust, which PREFIRE may be able to resolve after taking many measurements since the TIRS noise will be reduced by the square root of the number of measurements. Detecting diamond dust signatures would only be possible with the averaging of many TIRS observations. Beyond 30 μm, the sensitivities to different effective radii of diamond dust are extremely negligible. The difference between 2 and 12 μm of effective radius also yields negligible sensitivities across the spectrum with differences less than 0.1 K, indicating that PREFIRE would not be able to distinguish between effective radii for diamond dust.

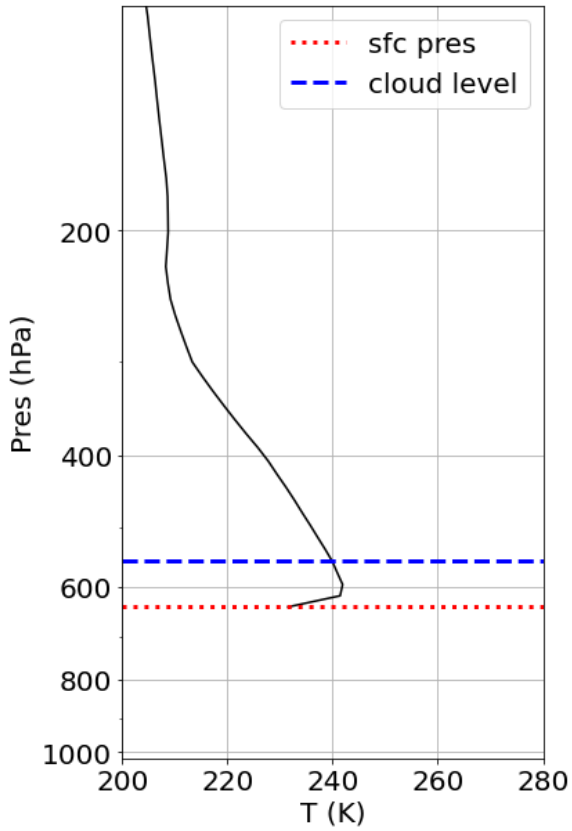

Figure 3.17. The temperature profile (black line) for Summit Station that shows the location of the low-level cloud (blue line) in the presence of an inversion.

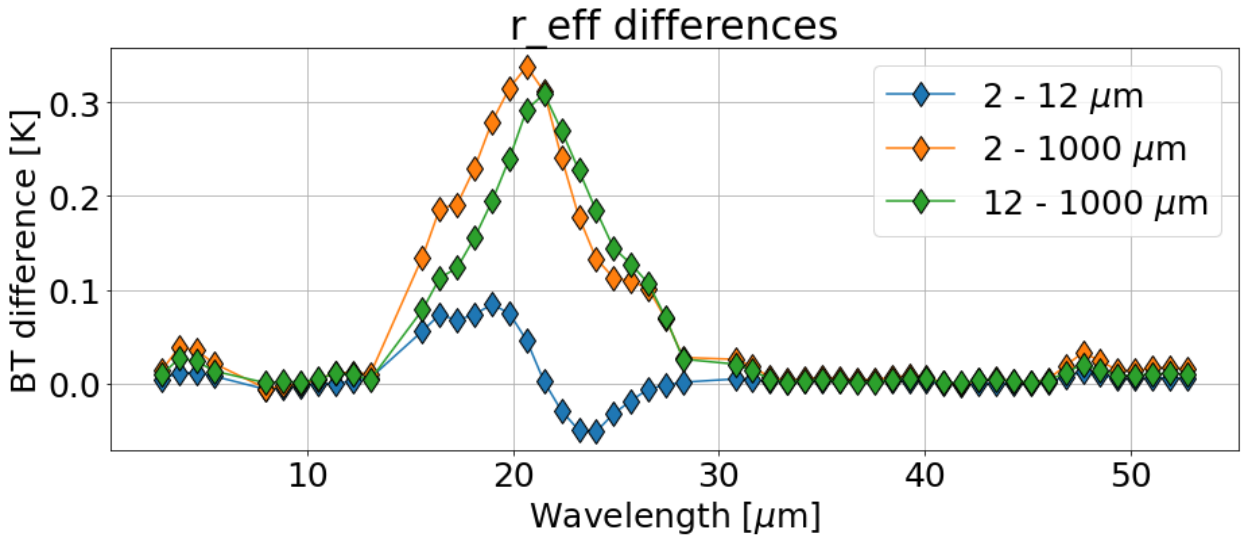

Figure 3.18. The differences in TIRS between 2, 12, and 1000 μm at Dome C II for low-level diamond dust during the austral summer.

Next, the diamond simulated at Dome C II will keep the effective radius constant at 12 μm, the average radius for diamond dust, and the OD is increased from 0.1 to 1. The result is shown in Figure 3.19.

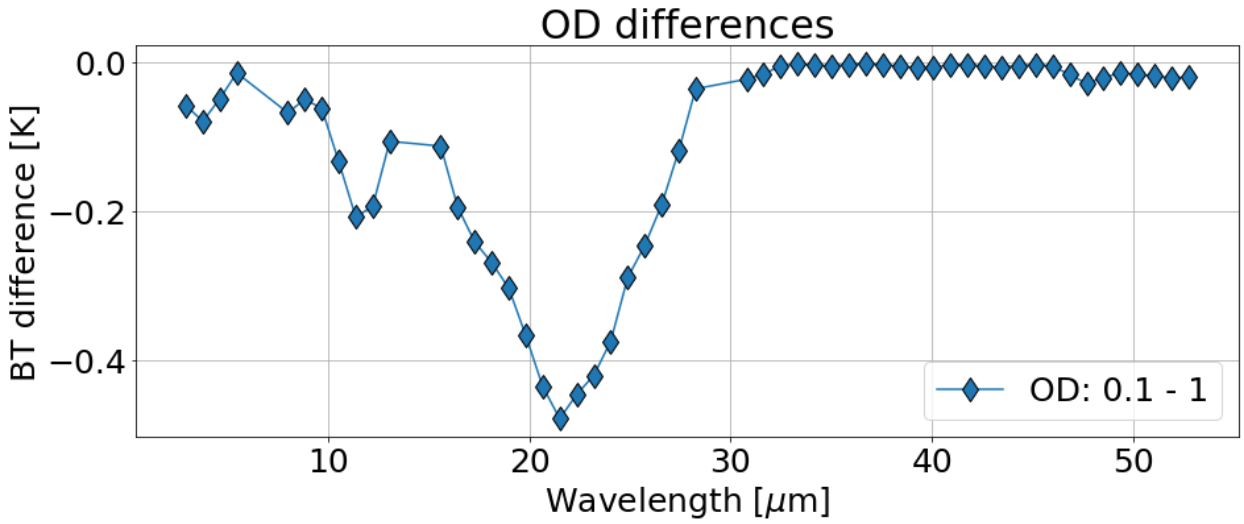

Figure 3.19. The differences in TIRS between ODs of 0.1 and 1 for low-level diamond dust during the austral winter at Dome C II.

The highest sensitivities to changing the OD of diamond dust at Dome C II occur in the dirty window channel just above 20 μm, but the sensitivities do not reach higher than 0.5 K in magnitude. This indicates that PREFIRE would most likely not be able to resolve such differences with just one measurement. Although the sensitivities are not large, if there was a satellite that could resolve such low TIRS differences, this result indicates that a diamond dust OD of 0.1 would cause less radiation to reach the satellite than an OD of 1, as all the differences across the spectrum are negative. Beyond 30 μm, the sensitivities are negligible. Next, similar simulations are done for each location for clouds in the mid-level atmosphere.

3.3.3 Mid-level clouds

For the following mid-level cloud simulations, each cloud is set at 5 km above the surface at each location. The first simulation considers mid-level liquid clouds at Dismal Island. The effective radius is changed between 5, 15, and 25 μm with a constant OD of 10, and the difference between each simulation is taken. The result is shown in Figure 3.20.

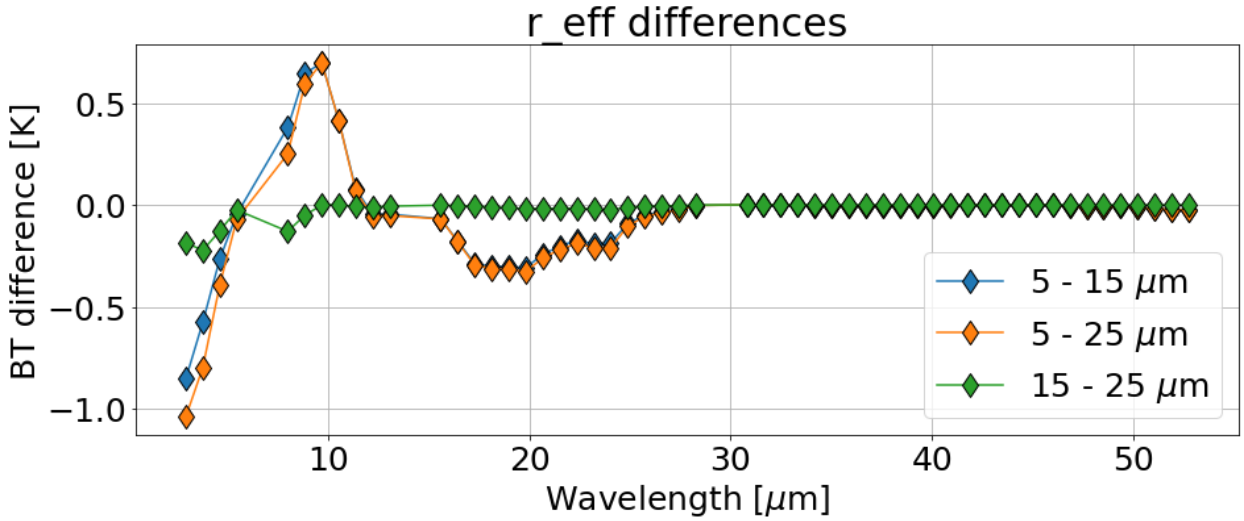

Figure 3.20. The differences in TIRS between effective radii of 5, 15, and 25 μm at Dismal Island for mid-level liquid clouds during the austral summer.

Mid-level liquid clouds at Dismal Island have a higher TIRS sensitivity to changing between the smaller radius of 5 μm and both the larger radii, as shown in the orange and blue lines in Figure 3.20. The sensitivities are similar in magnitude and occur in the same areas of the spectrum. Between effective radii of 5 μm and 15 μm, as well as 5 μm and 25 μm, sensitivities occur in the shorter wavelengths and have a difference of -1.0 K, just at the threshold of what PREFIRE can measure. In these shorter wavelengths, the TIRS differences are negative, indicating that an effective radius of 5 μm would yield less radiation reaching the satellite than the two higher radii. Around the ozone TIRS channel of 9.6 μm, the differences turn positive and are now around 0.7 K. With one PREFIRE measurement, this would most likely not be resolved, but with averaging numerous measurements, this sensitivity may be within PREFIRE's capabilities. This positive difference also tells us that the larger effective radii would cause more radiation to reach the satellite than the smaller radius of 5 μm. There are also some slight sensitivities between 5 μm and the other two radii that are less than 0.5 K in the dirty window channels, but these sensitivities will be negligible to PREFIRE. When comparing the two larger effective radii, 15 and 25 μm, the sensitivities do not reach above 0.5 K at any point throughout the TIRS spectrum, which indicates that PREFIRE will likely not be very sensitive to differences between larger effective radii for mid-level liquid clouds at Dismal Island.

The next simulation done at Dismal Island is for mid-level liquid clouds that have a constant effective radius of 15 μm, but the OD is changed between 10 and 30. The result is presented in Figure 3.21. There is only a measurable sensitivity to this change in liquid cloud OD at the shortest TIRS channel. This is because the infrared spectrum saturates at relatively low ODs, so the radiation received at the satellite remains the same as a cloud becomes thicker beyond an OD of 10. All these differences are positive, indicating that if a satellite could resolve the entire

spectrum, an OD of 10 would yield warmer brightness temperatures and thus more radiation reaching a satellite than an OD of 30. These differences do not reach higher than 0.1 K beyond the 4.6 μm TIRS channel, however, so it is not within the range that PREFIRE could resolve.

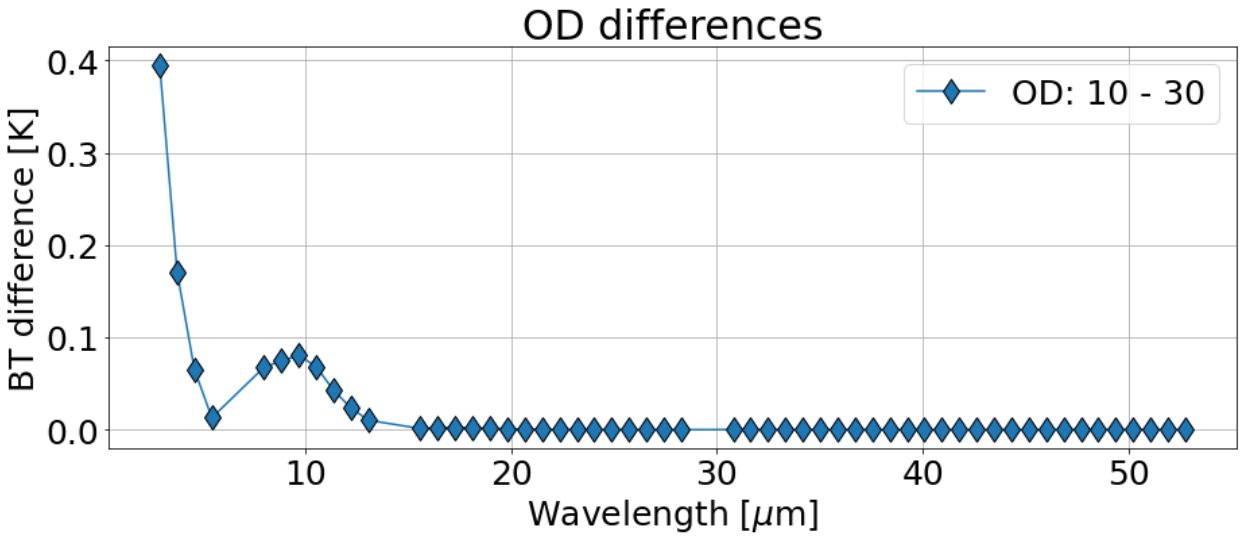

Figure 3.21. The differences in TIRS between ODs of 10 and 30 at Dismal Island for mid-level liquid clouds during the austral summer.

On the other hand, mid-level clouds over Summit Station, Greenland, which are likely composed entirely of ice, exhibit strong sensitivities to effective radius and OD changes, particularly in the far-infrared. Figure 3.22 shows a simulation where the effective radius of an ice cloud with a constant OD of 10 is changed between 5, 15, and 25 μm. The result is shown in Figure 3.22.

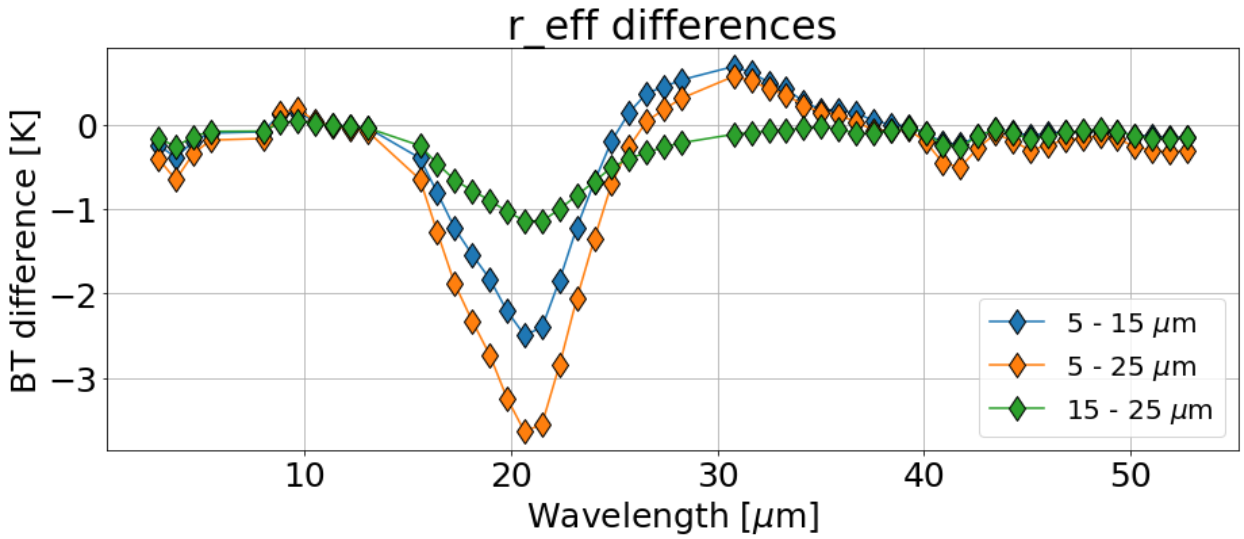

Figure 3.22. The differences in TIRS between effective radii of 5, 15, and 25 μm at Summit Station for mid-level ice clouds during the northern hemisphere winter.

There are sensitivities throughout the entire far-infrared spectrum that could be resolved by the PREFIRE TIRS for mid-level clouds at Summit Station. This discussion will begin by looking at the differences between an effective radius of 5 μm and the other two radii. The largest sensitivity occurs between 5 and 25 μm in the dirty window TIRS channels. The sensitivity reaches nearly -4.0 K, a difference that is well within the resolution of PREFIRE. Between effective radii of 5 and 15 μm, the TIRS differences decrease to about -2.5 K in the dirty window channels, still within PREFIRE's range. These negative differences indicate that the smaller effective radius of 5 μm will yield less radiation reaching the satellite than the two larger radii. When looking at the difference between 15 and 25 μm in the same dirty window region, the differences reach just past -1.0 K. This indicates that the larger the effective radius gets for mid-level ice clouds at Summit Station, the same the cloud looks to a TIRS measurement. Interestingly, the effect switches in the shorter water vapor channels of the TIRS channels between 25 and 35 μm where the differences between the 5 μm radius and the two larger radii are positive. This indicates that the smallest effective radius is now yielding warmer brightness temperatures and thus more radiation reaching

the satellite sensors in the shorter water vapor channels. A cloud with a smaller effective radius will also yield less radiation reaching the satellite in the shortest TIRS channels and in the water vapor channels, where the differences are also negative and range from -0.5 to 0 K. It is interesting that there are sensitivities in the TIRS channels beyond 30 μm, as these are the most novel measurements that are sensitive to ice cloud presence. As we move to the longest TIRS channels beyond 40 μm, the sensitivities decrease to less than 0.5 K, so PREFIRE will likely not be able to resolve effective radii differences in this part of the spectrum with one measurement, but it could be resolved with numerous measurements.

The next simulation keeps the effective radius constant at 15 μm and changes the cloud OD between 1 and 15 at Summit Station for mid-level ice clouds. The result is shown in Figure 3.23. The result shows sensitivities throughout the entire spectrum, and the differences are all positive, indicating that a cloud with an OD of 1 will result in higher brightness temperatures and thus more radiation reaching the satellite than an OD of 15. The highest sensitivities occur in the dirty window channel between TIRS channels of 20 and 25 μm. The difference is around 3.5 K, which can be discerned by PREFIRE. There are some sensitive TIRS channels around 10 μm as well, and these differences are greater than 1 K. As we look at the water vapor TIRS channels beyond 30 μm, there are some fluctuating sensitivities around 0.5 K, which indicates that PREFIRE may be sensitive to differing ODs for a mid-level ice cloud in the longer far-infrared wavelengths with many measurements, but not with a single measurement.

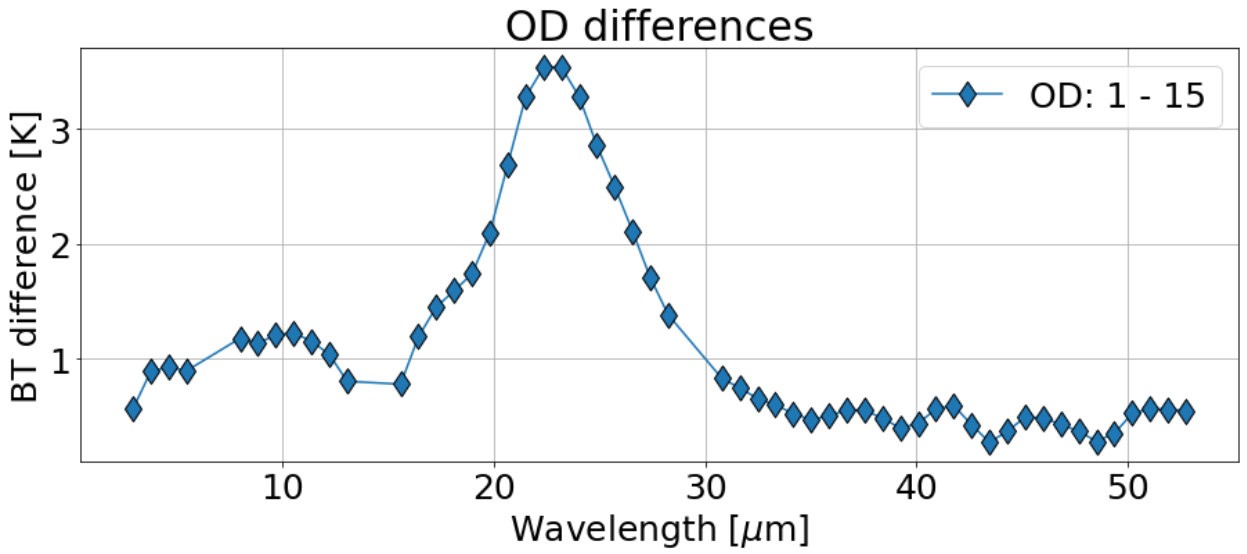

Figure 3.23. The differences in TIRS between ODs of 1 and 15 at Summit Station for mid-level ice clouds during the northern hemisphere winter.

Mid-level ice clouds at Dome C II are simulated next, where the sensitivities across the far-infrared spectrum decrease substantially. The first simulation done changes the effective radius between 5, 30, and 50 μm with a constant OD of 1. The result is shown in Figure 3.24.

There are differences throughout the entire spectrum that will be able to be resolved by PREFIRE. Between the effective radius of 5 μm and the two larger radii, there are positive differences in the shortest wavelengths that exceed 1.0 K. These positive differences indicate that the smaller radius will result in more radiation reaching the TIRS. Above TIRS channels of 10 μm but below 15 μm, the differences switch to be negative, which indicates that smaller radii will result in less radiation reaching the satellite. Beyond 15 μm, all of the differences are positive, with the largest sensitivities occurring between the cloud of a 5 μm effective radius and the two larger radii in the dirty window TIRS channels between 15 μm and 40 μm. In the dirty window channel, the differences are 4.0 K, well within PREFIRE's capabilities. Beyond 40 μm, the differences are less than 0.5 K which are negligible to PREFIRE's sensors with one measurement. When looking at the differences between the two larger effective radii of 30 and 50 μm, the differences do not

exceed 0.5 K throughout the entire far-infrared TIRS spectrum, meaning PREFIRE may be able to resolve such differences with many measurements, but not with just one measurement.

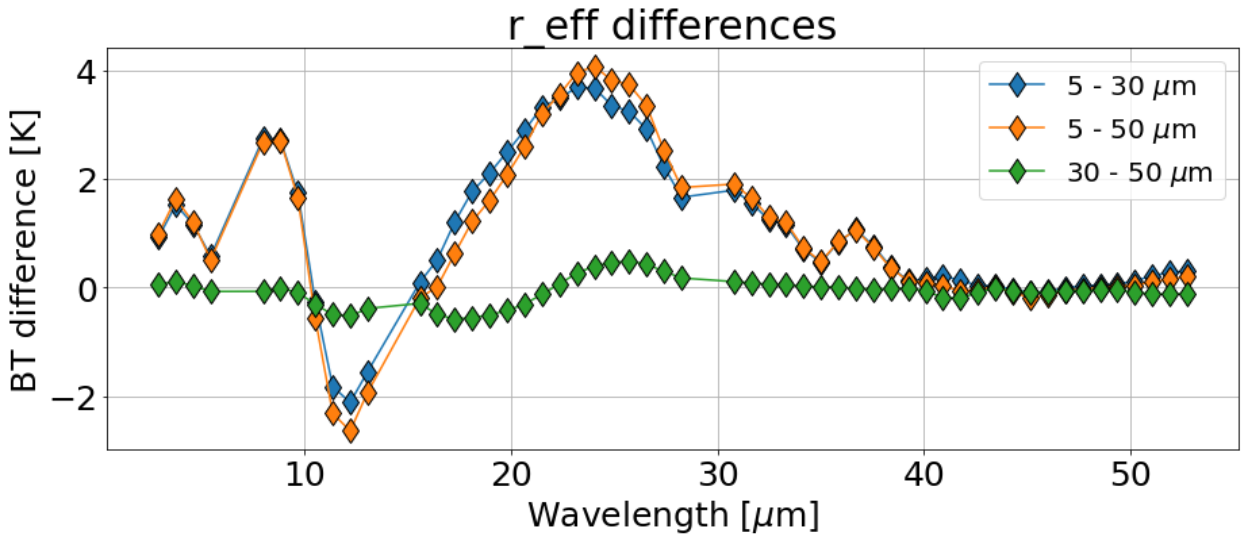

Figure 3.24. The differences in TIRS between effective radii of 5, 30, and 50 μm at Dome C II for mid-level ice clouds during the austral summer.

The next simulation done at Dome C II involves keeping the effective radius constant at 30 μm and changing the OD between 0.5 and 1. The result is shown in Figure 3.25. Across the entire far-infrared spectrum, this result yields TIRS differences less than 0.03 K, much less than PREFIRE's resolution even with many measurements. This result shows that changing between an OD of 0.5 to 1 for mid-level ice clouds at Dome C II will not produce a significant signal that could be discerned by PREFIRE. The final section for cloud sensitivities will simulate different types of high-level clouds at each location.

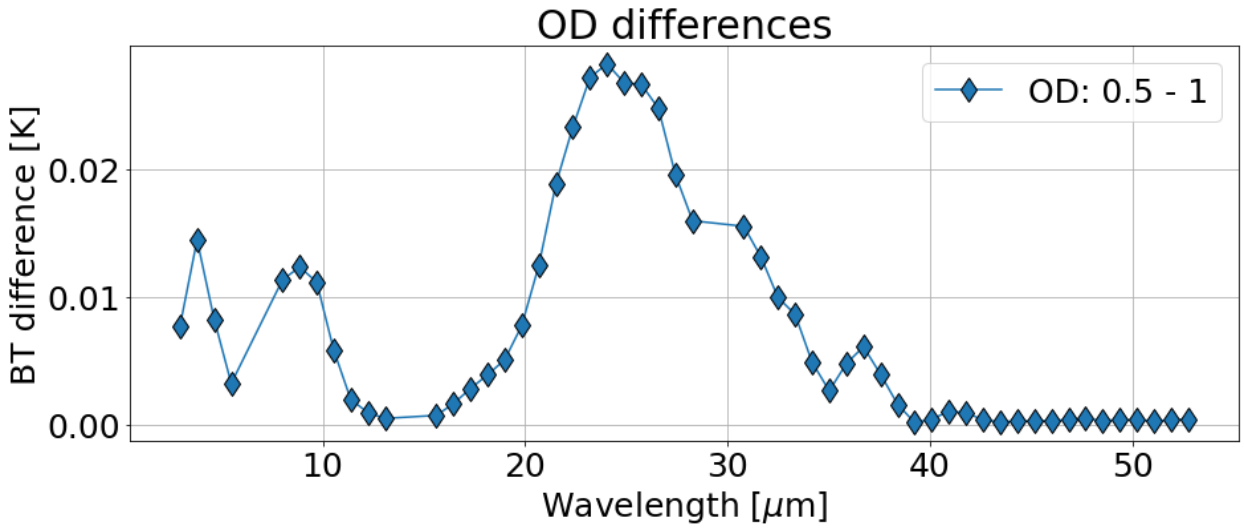

Figure 3.25. The differences in TIRS between ODs of 0.5 and 1 at Dome C II for mid-level ice clouds during the austral summer.

3.3.4 High-level clouds

For all the following high-level cloud simulations, the clouds are set as ice. The first simulation done for high-level clouds is at Dismal Island. Like the other Dismal Island cloud simulations, the effective radius is changed between 5, 15, and 25 μm, and the OD is kept constant at 10. This simulation is done for both the austral summer and winter, and the result is shown in Figure 3.26.

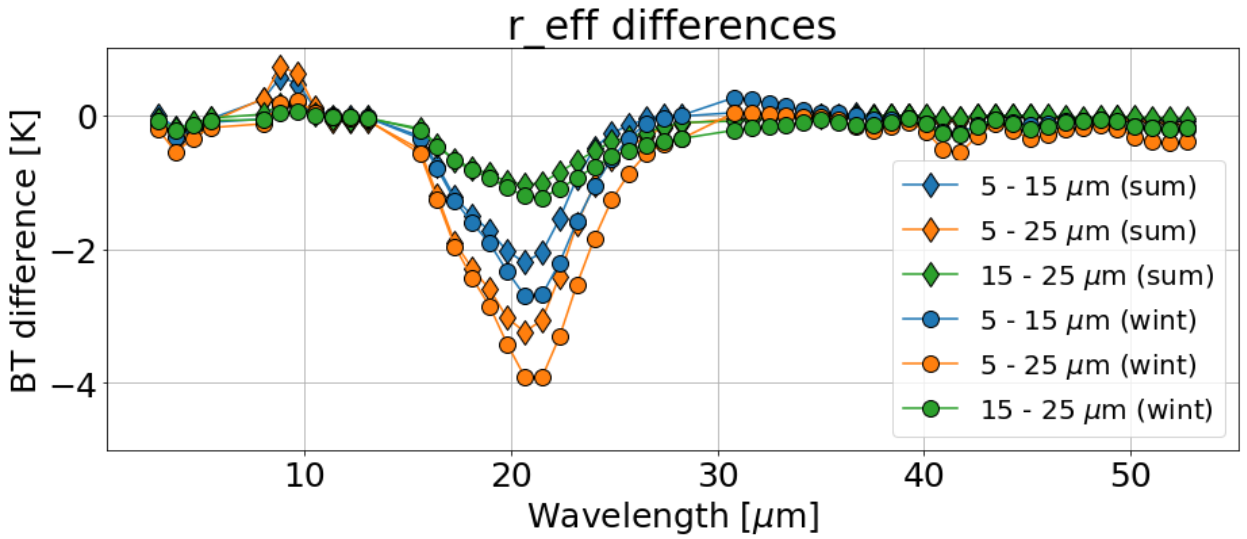

Figure 3.26. The differences in TIRS between effective radii of 5, 15, and 25 μm at Dismal Island for high-level ice clouds during the austral summer (diamond markers) and winter (circle markers).

Between summer and winter at Dismal Island, cirrus cloud signature differences between various effective radii will yield similar sensitivities across the far-infrared spectrum. This is similar to the result at Dismal Island for low-level clouds (Figure 3.13), where the sensitivities were also similar six months apart. In this simulation for cirrus clouds, the winter does appear to have a sensitivity slightly higher than the summer. This can be seen when looking at the largest sensitivity in the dirty window TIRS channels between effective radii of 5 and 25 μm. In the winter, the difference reaches -4.0 K whereas the summer difference maximum is -3.0 K. When looking at the difference in TIRS between effective radii of 5 and 15 μm, the winter maximum in the dirty window channel also has a slightly higher sensitivity than the summer. When comparing between radii of 15 and 25 μm, the differences are less than when compared with the smaller effective radius. In the dirty window channel, all the TIRS differences are negative, which indicates that smaller effective radii will yield less radiation reaching the satellite than larger effective radii. Beyond 30 μm, there are not many differences between differing effective radii. There is slight

sensitivity in the ozone TIRS channel of 9.6 μm between 5 μm and the two larger radii, where the difference reaches about 0.5 K, which could be identified by PREFIRE with many measurements. By comparing the summer and winter sensitivities to differing effective radii in this simulation, we can see that winter yields a slightly higher sensitivity, most likely due to less water vapor present influencing radiation reaching the satellite.

The next simulation involves keeping the effective radius constant at 15 μm over Dismal Island but changing between ODs of 10 and 30, again for both summer and winter. The result is shown in Figure 3.27. While there are some sensitivities across the spectrum, both summer and winter have TIRS differences less than 0.2 K, meaning that PREFIRE would not be able to resolve the difference between a high-level ice cloud of OD of 10 versus 30 at Dismal Island. Higher-resolution satellites may be able to resolve such a difference.

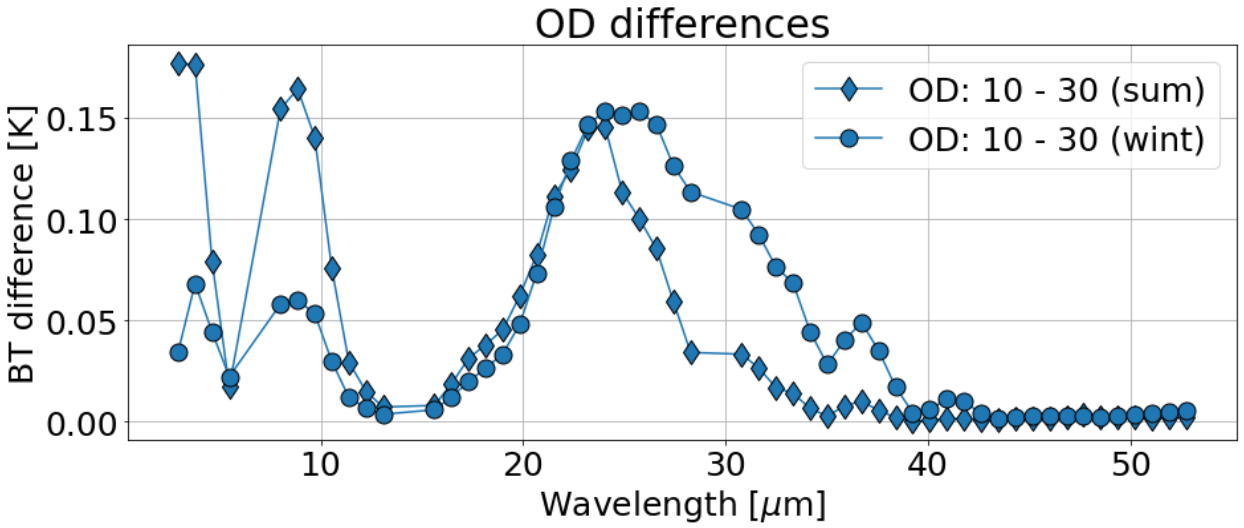

Figure 3.27. The differences in TIRS between ODs of 10 and 30 at Dismal Island for high-level ice clouds during the austral summer (diamond markers) and winter (circle markers).

At Summit Station, the cirrus clouds are simulated with effective radii changing between 5, 15, and 25 μm and with an OD constant of 10. The simulation is only done for the northern hemisphere winter, and the result is shown in Figure 3.28.

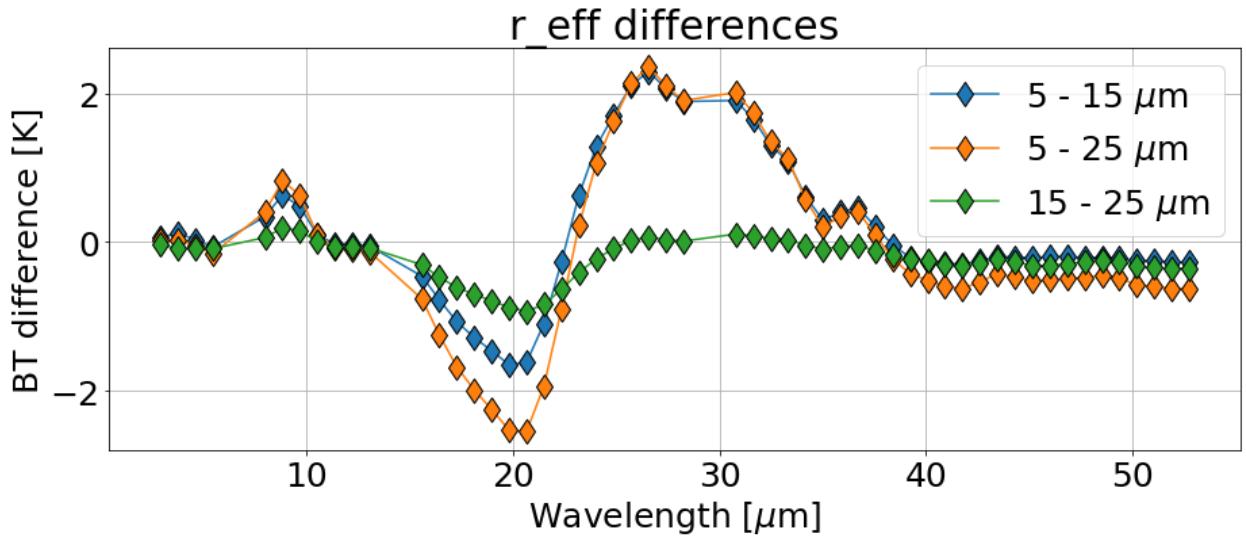

Figure 3.28. The differences in TIRS between effective radii of 5, 15, and 25 μm at Summit Station for high-level ice clouds during the northern hemisphere winter.

The highest sensitivity at Summit Station to changing effective radii occurs in the dirty window TIRS channels and some water vapor TIRS channels. The highest TIRS difference occurs around 20 μm between the smallest and largest radii of 5 and 25 μm. The sensitivity is around -2.5 K, a difference that PREFIRE would be able to resolve. This negative difference also indicates that the larger effective radius of 25 μm would yield more radiation reaching the satellite than the smaller radii. This result of a larger radius having a higher brightness temperature in the dirty window channel near 20 μm is also apparent when comparing effective radii of 15 and 25 μm and of 5 and 15 μm. The former yields a smaller difference in TIRS of nearly -1.0 K and the latter yields a difference of nearly -2.0 K. Interestingly, the TIRS spectrum behaves differently in the longer wavelengths of the dirty window channel and the beginnings of the water vapor channels, where the differences are now positive. This effect is likely attributed to the presence of this cloud in the stratosphere, where the temperature increases with height. As a result, TIRS channels from 22 to 40 μm exhibit sensitivity to different levels of the upper atmosphere than the TIRS channels from 15 to 22 μm. The smaller radius of 5 μm is now yielding more radiation reaching the satellite

than both the larger effective radii in the longer wavelengths of the dirty window channel. Both the differences between the 5 μm radius and the other two radii reach above 2.0 K, meaning PREFIRE will be able to resolve such differences. When looking at the difference between radii of 15 and 25 μm in this region of the spectrum, the differences do not exceed 0.5 K beyond 25 μm. In the longer water vapor channels, the differences between 5 and 25 μm do yield differences that are around 0.5 K, something that PREFIRE may be able to resolve with many measurements. There is also some sensitivity between the 5 μm radius and the other larger two radii in the ozone TIRS channel of 9.6 μm that nearly reach 1.0 K. This is also something that PREFIRE may be able to resolve.

At Summit Station, Greenland, the simulations for high-level clouds involve keeping the effective radius constant at 15 μm and changing the OD between 1 and 15. The result yields very large differences across the entire PREFIRE far-infrared spectrum, and the result is shown in Figure 3.29.

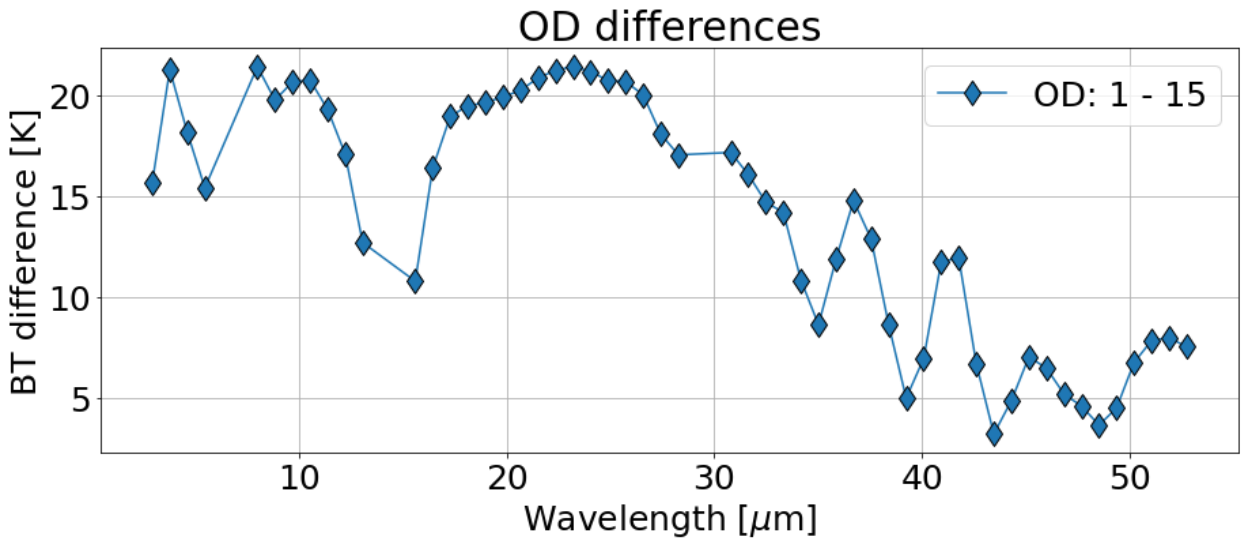

Figure 3.29. The differences in TIRS between ODs of 10 and 30 at Dismal Island for high-level ice clouds during the austral summer (diamond markers) and winter (circle markers).

Throughout the entire PREFIRE spectrum, the TIRS have a significant response to altering high-level cirrus clouds between ODs of 1 and 15. All the differences are positive, which indicates that high-level cirrus clouds with an OD of 1 would result in higher brightness temperatures than an OD of 15 and thus more radiation reaching the satellite at all TIRS channels. This is the opposite than what was found for low-level clouds at Summit Station with changing OD, where the differences were mostly negative (Figure 3.16). This is because the high-level cloud is set above the inversion (Figure 3.17), whereas the low-level cloud at this location was set within the inversion. At shorter wavelengths, transparent window channels, and dirty window channels, the maximum TIRS differences reach beyond 20 K. Even in the 15 μm CO_2 absorption channel, the difference is above 10 K, meaning these clouds are set above areas of high CO_2 concentration and thus influencing the TIRS retrievals at 15 μm. Beyond 30 μm, which contains the TIRS water vapor channels, the highest TIRS difference is around 15 K and lowest difference that occurs is around 4.0 K, which can both be distinguished by PREFIRE with just one measurement. This result is very interesting since it tells us that every TIRS channel is sensitive above 1 K to an OD change between 1 and 15 of a high-level cirrus cloud at Summit Station, which ultimately tells us that PREFIRE should be able to discern these OD differences.

The final part of this section involves simulating polar stratospheric clouds over Dome C II. These clouds are set at 25 km above the surface. The effective radius is changed between 1, 5, and 10 μm while the OD stays constant at 1. The result is shown in Figure 3.29.

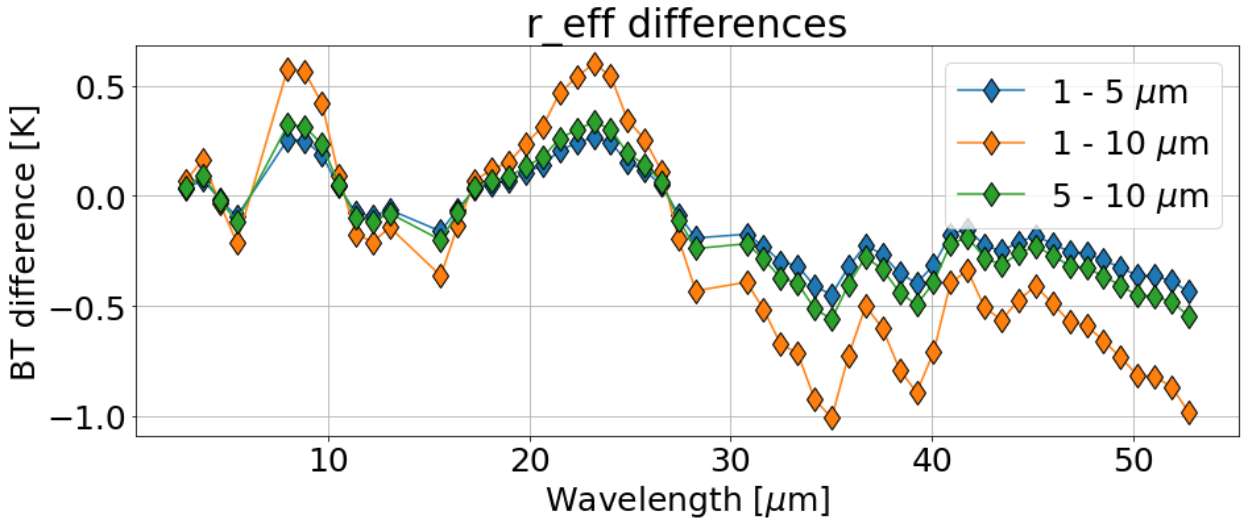

Figure 3.29. The differences in TIRS between effective radii of 1, 5, and 10 μm at Dome C II for polar stratospheric clouds in the austral summer.

This result shows the highest sensitivity to changing effective radius of polar stratospheric clouds between 1, 5, and 10 μm occurs in the water vapor channel. The maximum differences in TIRS brightness temperature are found when looking at the difference between effective radii of 1 and 10 μm in the water vapor channel. The largest differences of -1.0 K occur at the 35.0 μm and the 52.7 μm TIRS channels, which indicates that an effective radius of 10 μm will result in significantly warmer brightness temperatures and thus more radiation reaching the satellite than an effective radius of 1 μm. When analyzing the differences between the 5 μm effective radius and the other two radii, there are also differences in the water vapor TIRS channels with similar maxima of -0.5 K at TIRS channels of 35.0, 39.2, and 52.7 μm. In the dirty window channel, there is sensitivity at the 24.0 μm TIRS channel to effective radius differences between 1 and 10 μm and it reaches over 0.5 K, which may be distinguishable by PREFIRE with many measurements. There is similar sensitivity in the 9.6 μm ozone channel, and both differences are positive which indicates that polar stratospheric clouds with an OD of 1 will have higher brightness temperatures and thus more radiation reaching a satellite than an OD of 10 over Dome C II. Throughout the rest of the

spectrum at TIRS channels less than 30 μm, and other than the 1 and 10 μm differences, the sensitivities are less than 0.5 K, which may not be distinguishable by PREFIRE even with many measurements.

The final simulation done in this section is for polar stratospheric clouds over Dome C II, and the effective radius is now set at a constant 5 μm while the OD is changed between 0.1 and 1. The result is shown in Figure 3.30.

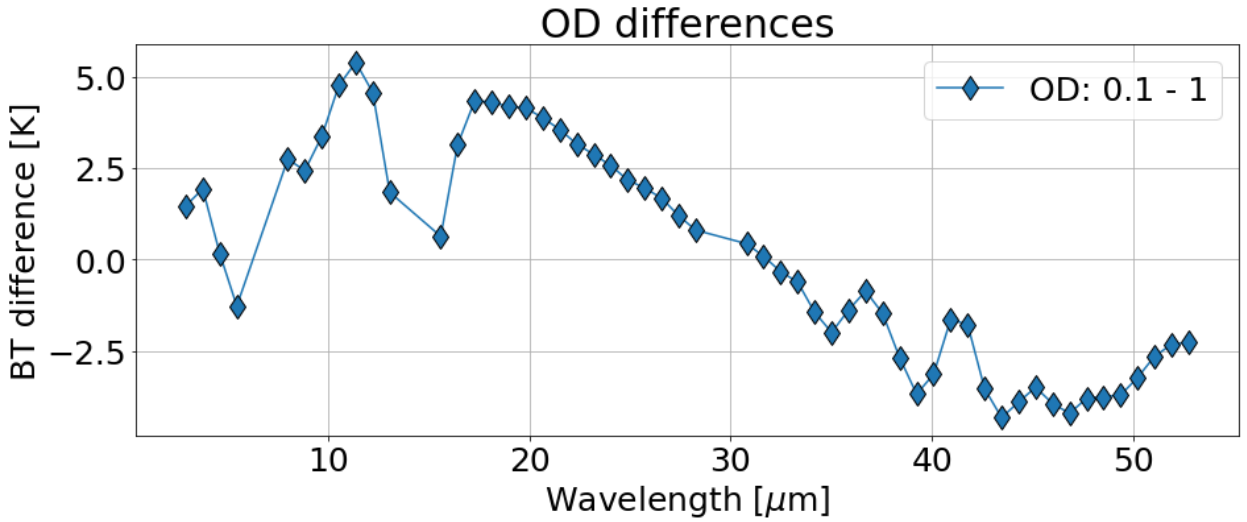

Figure 3.30. The differences in TIRS between ODs of 0.1 and 1 at Dome C II for polar stratospheric clouds during the austral summer.

There are significant differences in TIRS measurements when comparing ODs of 0.1 and 1 for polar stratospheric clouds over Dome C II. The highest sensitivity occurs in the transparent window channel of 11.4 μm with a TIRS difference over 5.0 K. There is also high sensitivity in the dirty window channel between 16 and 30 μm, where the difference in TIRS outputs is nearly 5.0 μm near the 16 μm TIRS channel and then decreases to about 1.0 K at the 28.2 μm TIRS channel. Before 30 μm, most differences, apart from the 5.5 μm TIRS channel, are positive, indicating that an OD of 0.1 for a polar stratospheric cloud would yield higher brightness temperatures and thus more radiation reaching the satellite than an OD of 1. Beyond 30 μm, the

TIRS channel differences become negative, but nearly reach a difference of -5.0 K in the water vapor channels. This indicates that a polar stratospheric cloud with an OD of 0.1 would now yield colder brightness temperatures and thus less radiation reaching the satellite in the water vapor channels. Throughout the far-infrared spectrum, changing ODs between 0.1 and 1 of polar stratospheric clouds will result in large differences above 1.0 K in many parts of the spectrum, which PREFIRE will be able to resolve.

3.3.5 Cloud sensitivity summary

Cloud presence, cloud phase, altering effective radii, and altering ODs was explored in this section. Optically thin ice clouds are of particular interest due to how the far-infrared spectrum is very sensitive to them. Dry areas like Dome C II and Summit Station exhibited significant sensitivity to ice cloud presence in the mid-level atmosphere of 5 km above the surface, while dirty window channels displayed sensitivity to cloud phase and transparent window channels displayed minimal sensitivity. Water vapor channels were sensitive to cloud presence and phase, especially in dry regions. When simulating low-level clouds at each location, there was varying TIRS sensitivity with Dismal Island and Summit Station being more sensitive to changing effective radius than Dome C II. High-level ice clouds, including polar stratospheric clouds at Dome C II, showed TIRS sensitivity to changing effective radii, while Dismal Island experienced negligible differences in TIRS for changing OD. The other two locations showed significant TIRS sensitivities across the spectrum for changing ODs. Inversions also impacted cloud detection, which was explored particularly at Summit Station, where the inversion caused clouds with larger ODs to have more radiation reaching the satellite than the thinner cloud of smaller OD due to the cloud’s position at the top of the inversion in a warmer area than the surface. These findings

highlight the unique sensitivities of far-infrared TIRS measurements to varying cloud types at three different polar locations.

4 Conclusion

This thesis provides a pre-launch analysis for the PREFIRE satellite mission, launching in 2024, to determine what kinds of polar atmospheric conditions will produce the highest TIRS sensitivity. Understanding emitted radiation in polar regions, particularly in the far-infrared portion of the longwave spectrum, is crucial to gain an insight into how polar temperatures, snow cover, polar albedo, and sea ice are changing in the twenty-first century. Three different PREFIRE simulations were conducted to predict the sensitivity of the TIRS measurements: the annual cycle (including inversion presence), surface type changes, and cloud presence. These simulations were done using PCRTM over three specific locations where there is surface observational data through either the AMRDC network (Dismal Island and Dome C II) or the ICECAPS project (Summit Station).

In the first simulation, general clear-sky characteristics of the PREFIRE TIRS measurements are simulated on an annual timescale. Exploring PREFIRE's responses to annual polar conditions is important to fully characterize global radiation, as the poles act as a sink to the excess radiation that they receive from solar input and from global transport. It was found that Dismal Island experiences the least variability throughout the far-infrared spectrum, which is a result of the warm and moist conditions at this location, causing the far-infrared spectrum to be heavily influenced by water vapor. At Dome C II, the highest variability and coldest TIRS temperatures were observed, and inversions caused the transparent window channel brightness temperatures to be colder than brightness temperatures in the water vapor channels. This location experiences the least water vapor present, so the TIRS vary considerably throughout an annual cycle. Summit Station yielded results between these two extremes. It is a warmer location than Dome C II, but it is drier than Dismal Island, so it experiences more variability than Dismal Island

but less than Dome C II. It also experienced inversions, but not as strong as the ones found at Dome C II.

Changes in surface emissivity were explored in the next section of simulations, which are significant considering how each unique surface – fine snow, medium snow, ice, and water – exhibits varying emissivities at different wavelengths in the far-infrared. Polar regions are unique in that they are very dry, meaning that in clear-sky conditions, there would not be extensive water vapor presence to influence PREFIRE's ability to measure surface conditions and distinguish between differing surface types. The potential impact of katabatic winds on surface emissivity was also explored in this section, considering their potential to induce snow-type changes. It was found that the transparent and dirty window channels are most sensitive to surface emissivity changes, and water vapor channels are much less sensitive. The sensitivity of the TIRS depends on the surface emissivity differences, as well as the transparency of the atmosphere. The snow type changing at Dome C II produced the least sensitivity of TIRS, and the water surface changing into an ice surface at Dismal Island produced the most sensitivity of TIRS in the transparent window channels.

The effect of cloud presence and changing cloud types in terms of phase and level was explored in the final simulations. Although many cloud types are explored in the results section, optically thin ice clouds are of particular interest due to how the far-infrared spectrum is very sensitive to their presence. It was found that dry areas like Dome C II and Summit Station will be very sensitive to ice cloud presence in the mid-level atmosphere, even for clouds with small ODs. Dirty window channels will be very sensitive to cloud phase, and transparent window channels will not be very sensitive to cloud phase. Water vapor channels are sensitive to cloud presence and cloud phase, more so in dry areas like Dome C II and Summit Station. When looking at low-level

clouds, Dismal Island and Summit Station will have more TIRS sensitivity across the spectrum when changing effective radius than Dome C II. Each location was found to be sensitive within PREFIRE's threshold to clouds in the mid-level atmosphere. While Dismal Island did not have significant sensitivities in the longer wavelength water vapor channels to either changing effective radius or OD, Summit Station and Dome C II experienced sensitivities, especially in the dirty window channels and the shorter wavelength water vapor channels. Changing ODs of low-level clouds at Dismal Island and diamond dust Dome C II did not yield very large TIRS sensitivities. All locations experience TIRS sensitivity to changing effective radii of high-level ice clouds, including polar stratospheric clouds at Dome C II. Only Dismal Island experiences negligible differences in TIRS for changing the OD between 10 and 30. The other two locations experience significant TIRS sensitivities across the spectrum when changing ODs between 1 and 15 of high-level ice clouds over Summit Station and between 0.1 and 1 of high-level polar stratospheric clouds over Dome C II. Inversions also caused an impact on cloud presence, especially at Summit Station, which experienced an inversion during these cloud simulations. The inversion caused the cloud with a larger OD to have more radiation reaching the satellite than a cloud with a smaller OD, and this is because the cloud was set in the vicinity of an inversion in an area that was warmer than the surface temperature.

Studying far-infrared radiation in polar climates and simulating data for various atmospheric and surface conditions is essential for our full comprehension of the Earth's global energy balance and the ever-evolving polar climate. By investigating the sensitivities of the PREFIRE TIRS of the annual cycle, inversions, surface emissivity changes, and cloud presence, we can predict the PREFIRE TIRS' response to various radiative properties in different polar conditions.

5 Future work

It is important to note that all the simulations done in this project are for the pre-launch PREFIRE TIRS measurements. These simulations have not been compared to real data, as there is no real PREFIRE data yet. After the mission launches, these simulations can be compared to real data in order to be validated.

The simulations presented in this project can also be converted into an algorithm in the future, which could then be applied to real PREFIRE data so that the mission can quickly identify inversions, surface emissivity changes, and cloud presence. Furthermore, the AWS in Antarctica may add on far-infrared sensors that will measure either broadband or spectrally resolved radiation. The AMRDC AWS network is already a very useful data network in Antarctica that can be used to validate surface measurements taken by PREFIRE through transparent window TIRS channels, and if far-infrared sensors were installed to each AWS, the validations could be enhanced.

Finally, any future satellite missions after PREFIRE (for example, FORUM and TICFIRE) that measure into the far-infrared may be able to resolve TIRS sensitivities of less than 1 K with one measurement, so all the simulations that had TIRS signature difference of less than 1 K could potentially be discerned with a higher-spectral resolution satellite.

References

Ackerman, S. A., and Coauthors, 2019: Satellites see the world's atmosphere. *A Century of Progress in Atmospheric and Related Sciences: Celebrating the American Meteorological Society Centennial, Meteor. Monogr., No. 59*, Amer. Meteor. Soc., https://doi.org/10.1175/AMSMONOGRAPHS-D-18-0009.1.

Ahlenius, Hugo. (2008) Major Research Stations in the Arctic. *UNEP/GRID-Arendal*, Retrieved May 10, 2023, from http://www.grida.no/graphicslib/detail/major-research-stations-in-the-arctic_ad9b#

AMRDC. (2022). Automatic Weather Stations - 2022. *Space Science & Engineering Center, UW-Madison*. Retrieved May 10, 2023, from https://amrc.ssec.wisc.edu/aws/index.php

Box, J. E., Fettweis, X., Stroeve, J. C., Tedesco, M., Hall, D. K., & Steffen, K. (2012). Greenland ice sheet albedo feedback: Thermodynamics and atmospheric drivers. The Cryosphere, 6(4), 821–839. https://doi.org/10.5194/tc-6-821-2012.

Bumbaco, K. A., Hakim, G. J., Mauger, G. S., Hryniw, N., & Steig, E. J. (2014). Evaluating the Antarctic Observational Network with the Antarctic Mesoscale Prediction System (AMPS), *Monthly Weather Review*, *142*(10), 3847-3859. Retrieved Jan 5, 2023, from https://journals.ametsoc.org/view/journals/mwre/142/10/mwr-d-13-00401.1.xml

Chen, Y.-H., 2020: *Influences of surface spectral emissivity and cloud longwave scattering on climate simulations*. Ph.D. thesis, University of Michigan at Ann Arbor, 160 pp.

Conrath, B. J., R. A. Hanel, V. G. Kunde, and C. Prabhakara, 1970: The Infrared Interferometer

Experiment on Nimbus 3. *J. Geophys. Res.*, **75**, 5831–5857, https://doi.org/10.1029/JC075i030p05831.

Eayrs, C., Holland, D. M., Francis, D., Wagner, T. J. W., Kumar, R., & Li, X. (2019). Understanding the seasonal cycle of Antarctic sea ice extent in the context of longer-term variability. Reviews of Geophysics, 57, 1037-1064. https://doi.org/10.1029/2018RG000631

Groot Zwaaftink, C. D., Cagnati, A., Crepaz, A., Fierz, C., Macelloni, G., Valt, M., and Lehning, M.: Event-driven deposition of snow on the Antarctic Plateau: analyzing field measurements with SNOWPACK, The Cryosphere, 7, 333–347, https://doi.org/10.5194/tc-7-333-2013, 2013.

Hall, D. K., Comiso, J. C., DiGirolamo, N. E., Shuman, C. A., Box, J. E., and Koenig, L. S. (2013), Variability in the surface temperature and melt extent of the Greenland ice sheet from MODIS, *Geophys. Res. Lett.*, 40, 2114– 2120, doi:10.1002/grl.50240.

Hanel, R. A., B. Schlachman, F. D. Clark, C. H. Prokesh, J. B. Taylor, W. M. Wilson, and L. Chaney, 1970: The Nimbus III Michelson interferometer. *Appl. Opt.*, **9**, 1767–1774, https://doi.org/10.1364/AO.9.001767.

Harries, J., Carli, B., Rizzi, R., Serio, C., Mlynczak, M., Palchetti, L., Maestri, T., Brindley, H., and Masiello, G. (2008), The far-infrared Earth, *Rev. Geophys.*, 46, RG4004, doi:10.1029/2007RG000233.

Hersbach, H., and Coauthors, 2020: The ERA5 global reanalysis. Quarterly Journal of the Royal Meteorological Society, 146 (730), 1999–2049, https://doi.org/https://doi.org/10.1002/qj.3803, URL https://rmets.onlinelibrary.wiley.com/doi/abs/10.1002/qj.3803.

Huang, X. L., X. H. Chen, D. K. Zhou, and X. Liu, 2016: An observationally based global band-by-band surface emissivity dataset for climate and weather simulations. *J. Atmos. Sci.*, **73**, 3541–3555, https://doi.org/10.1175/JAS-D-15-0355.1.

Huang, X. L., X. H. Chen, G. L. Potter, L. Oreopoulos, J. N. S. Cole, D. M. Lee, and N. G. Loeb, 2014: A global climatology of outgoing longwave spectral cloud radiative effect and associated effective cloud properties. *J. Climate*, **27**, 7475–7492, https://doi.org/10.1175/JCLI-D-13-00663.1.

Irannezhad, Masoud & Ahmadi, Behzad & Marttila, Hannu. (2022). Impacts of climate extremes over Arctic and Antarctic Climate Impacts on Extreme Weather, 191-215. 10.1016/B978-0-323-88456-3.00004-6.

Konzelmann, T., & Ohmura, A. (1995). Radiative fluxes and their impact on the energy balance of the Greenland ice sheet. *Journal of Glaciology*, *41*(139), 490-502. doi:10.3189/S0022143000034833.

Lachlan-Cope T. (2010). Antarctic clouds. *Polar Research, 29*(2), 150-158. https://doi.org/10.3402/polar.v29i2.6065

Lacour, A., Chepfer, H., Miller, N. B., Shupe, M. D., Noel, V., Fettweis, X., Gallee, H., Kay, J. E., Guzman, R., & Cole, J. (2018). How Well Are Clouds Simulated over Greenland in Climate Models? Consequences for the Surface Cloud Radiative Effect over the Ice Sheet, *Journal of Climate*, *31*(22), 9293-9312. doi: https://doi.org/10.1175/JCLI-D-18-0023.1

Lazzara, M. A., G. A. Weidner, L. M. Keller, J. E. Thom, and J. J. Cassano, 2012: Antarctic Automatic Weather Station Program: 30 Years of Polar Observation. *Bull. Amer. Meteor. Soc.*, **93**, 1519–1537, https://doi.org/10.1175/BAMS-D-11-00015.1.

L'Ecuyer, T. S., and Coauthors, 2015: The observed state of global energy balance in the early

21st century. *J. Climate*, **28**, 8319–8346, https://doi.org/10.1175/JCLI-D-14-00556.1.

L'Ecuyer, T. S., Drouin, B. J., Anheuser, J., Grames, M., Henderson, D. S., Huang, X., Kahn, B. H., Kay, J. E., Lim, B. H., Mateling, M., Merrelli, A., Miller, N. B., Padmanabhan, S., Peterson, C., Schlegel, N., White, M. L., & Xie, Y. (2021). The Polar Radiant Energy in the Far Infrared Experiment: A New Perspective on Polar Longwave Energy Exchanges, *Bulletin of the American Meteorological Society*, *102*(7), E1431-E1449. doi: https://doi.org/10.1175/BAMS-D-20-0155.1

Libois, Q., Ivanescu, L., Blanchet, J.-P., Schulz, H., Bozem, H., Leaitch, W. R., et al. (2016). Airborne observations of far-infrared upwelling radiance in the Arctic. Atmospheric Chemistry and Physics, 16, 15689-15707. doi:10.5194/acp-16- 15689-2016.

Liu, X., Zhou, D. K., Larar, A. M., Smith, W. L., Schluessel, P., Newman, S. M., Taylor, J. P., and Wu, W.: Retrieval of atmospheric profiles and cloud properties from IASI spectra using super-channels, Atmos. Chem. Phys., 9, 9121–9142, https://doi.org/10.5194/acp-9-9121-2009, 2009.

Liu, X., Smith, W. L., Zhou, D. K., & Larar, A. (2006). Principal component-based radiative transfer model for hyperspectral sensors: Theoretical concept. Applied Optics, 45 (1), 201–209. https://doi.org/10.1364/AO.45.000201

Mahesh A., Walden V.P. & Warren S. 2001b. Ground-based remote sensing of cloud properties over the Antarctic Plateau. Part II: cloud optical depths and particle sizes. Journal of Applied Meteorology 40, 1279–1294

McClatchey, R. A., R. W. Fenn, J. E. A. Selby, F. E. Volz, and J. S. Garing, 1972: Optical properties of the atmosphere. Rep. AFCRL-72-0497, Hanscom Air Force Base, Bedford, Mass., 110 pp

Meier, W. N., et al. (2014), Arctic sea ice in transformation: A review of recent observed changes and impacts on biology and human activity, Rev. Geophys.,51,185–217, doi:10.1002/2013RG000431

Miller, N. B., Merrelli, A., L'Ecuyer, T. S., & Drouin, B. J. (2023). Simulated Clear-Sky Water Vapor and Temperature Retrievals from PREFIRE Measurements, *Journal of Atmospheric and Oceanic Technology* (published online ahead of print 2023). doi: https://doi.org/10.1175/JTECH-D-22-0128.1

NOAA. (n.d.). *ICECAPS observatory at Summit Station, Greenland*. Physical Sciences Laboratory. https://psl.noaa.gov/arctic/observatories/summit/

Palchetti, L., Brindley, H., Bantges, R., Buehler, S., Camy-Peyret, C., Carli, B., et al. (2020). FORUM: Unique far-infrared satellite observations to better understand how Earth radiates energy to space. Bulletin of the American Meteorlogical Society, 101(12), E2030-E2046. doi: 10.1175/BAMS-D-19-0322.1.

Parkinson C. L. (2019). A 40-y record reveals gradual Antarctic sea ice increases followed by decreases at rates far exceeding the rates seen in the Arctic. *Proceedings of the National Academy of Sciences of the United States of America*, *116*(29), 14414–14423. https://doi.org/10.1073/pnas.1906556116

Pettersen, C., Bennartz, R., Merrelli, A. J., Shupe, M. D., Turner, D. D., and Walden, V. P.: Precipitation regimes over central Greenland inferred from 5 years of ICECAPS observations, Atmos. Chem. Phys., 18, 4715–4735, https://doi.org/10.5194/acp-18-4715-2018, 2018.

Picard, G., Royer, A., Arnaud, L. and Fily, M. (2013): Influence of meter-scale wind-formed

features on the variability of the microwave brightness temperature around Dome C in Antarctica. The Cryosphere Discuss., 7, 3675-3716, doi:10.5194/tc-8-1105-2014.

Scambos, T. A., Campbell, G. G., Pope, A., Haran, T., Muto, A., Lazzara, M., et al. (2018).

Ultralow surface temperatures in East Antarctica from satellite thermal infrared mapping: The coldest places on Earth. *Geophysical Research Letters*, 45, 6124– 6133. https://doi.org/10.1029/2018GL078133

Spankuch, D. & Döhler, W. (1985). Radiative properties of cirrus clouds in the middle IR

derived from Fourier spectrometer measurements from space. Zeitschrift für Meteorologie, 35 (6). 314-324

Stone R.S. 1993. Properties of austral winter clouds derived from radiometric profiles at the South Pole. Journal of Geophysical Research—Atmospheres 98, 12 961–12 971.

Timofeev, Y.M., Polyakov, A.V., Kozlov, D.A., Zavelevich, F.S., Golovin, Y.M., Döhler, W.,

Oertel, D., & Spankuch, D. (2019). Comparison between the spectra of outgoing infrared radiation for different years. Izvestiya, Atmospheric and Oceanic Physics, 55, 956-962. doi: 10.1134/S0001433819090524

Turner, J. (2015). ARCTIC AND ANTARCTIC | Antarctic Climate. *Encyclopedia of*

Atmospheric Sciences (Second Edition), 98-106. https://doi.org/10.1016/B978-0-12-382225-3.00044-X

Walsh, J.E. 2013. Melting ice: What is happening to Arctic sea ice, and what does it mean for

us? *Oceanography* 26(2):171–181, https://doi.org/10.5670/oceanog.2013.19.